Precambrian Research xxx (2016) xxx-xxx

Contents lists available at ScienceDirect

Precambrian Research

journal homepage: www.elsevier.com

Palaeoproterozoic assembly of the São Francisco craton, SE Brazil: New insights from U–Pb titanite and monazite dating

Carmen Aguilar [a, *], Fernando F. Alkmim [a], Cristiano Lana [a], Federico Farina [a, b]

[a] *Applied Isotope Research Group, Departamento de Geologia, Universidade Federal de Ouro Preto, Campus Universitário Morro do Cruzeiro s/n, 35400-000 Ouro Preto, MG, Brazil*

[b] *Department of Earth and Environmental Science, University of Geneva, Rue des Maraîchers 13, 1205 Geneva, Switzerland*

ARTICLE INFO

Article history:
Received 19 July 2016
Received in revised form 8 December 2016
Accepted 10 December 2016
Available online xxx

Keywords:
Southern São Francisco craton
Titanite
Monazite
syn-collisional metamorphism
Slow cooling
Palaeoproterozoic orogen

ABSTRACT

Isotopic U–Pb titanite and monazite data from the southern São Francisco craton better constrain the timing of the tectono-thermal event that led to the amalgamation of the craton and the crust that forms the basement of its fringing orogenic belts in the Palaeoproteroic. The data obtained from assemblages exposed in the Quadrilátero Ferrífero mining district and adjacent Palaeoproterozoic Mineiro belt magmatic arc terrane reveal two different age populations: a first metamorphic event between 2772 and 2613 Ma, followed by recrystallization or/and isotopic resetting in the interval of 2080–1940 Ma. The partial preservation of Neoarchaean ages in the craton interior suggests that the Palaeoproterozoic metamorphism did not exceed the minimum closure temperature for the titanite (between 650 °C and 700 °C), which is also reinforced by the absence of Palaeoproterozoic metamorphic zircons in the southern São Francisco craton. Combining new and existing Palaeoproterozoic data, we infer that the Archaean crust of the southern craton as well as the surrounding magmatic arcs were affected by a long-lived metamorphic event from *ca.* 2100 Ma to 1940 Ma. These age interval includes an episode of syn-collisional metamorphism between 2100 and 2070 Ma, which represents the amalgamation of the Archaean nuclei of both the São Francisco and Congo cratons, along with magmatic arcs and micro-continents. This collision led to closure of the large Palaeoproterozoic Minas basin, followed by orogenic collapse and development of a dome-and-keel architecture in time interval of 2070–2050 Ma. A period of slow cooling (~1 °C/Ma) succeeded these events and lasted until *ca*. 1940 Ma. Our results correlate with the Palaeoproterozoic metamorphic ages obtained in the various blocks forming the northeastern sector of the craton.

1. Introduction

Understanding the assembly of the crust that makes up the São Francisco Craton (SFC) and its margins in southeast Brazil has important implications for modeling the crustal evolution of the South American lithosphere. The SFC is surrounded by Late Edicaran-Cambrian Brasiliano orogenic belts, which define its boundaries. The craton contains some of the oldest Archaean kernels of South America and its crust extends further into the surrounding Brasiliano belts, forming a substantial part of their basement. The old kernels have been shielded from significant magmatic and tectonic overprint since *ca.* 1900 Ma (Almeida, 1977; Almeida et al., 1981; Teixeira et al., 2000; Alkmim, 2004; Barbosa and Sabaté, 2004; Alkmim and Martins-Neto, 2012). The Palaeoproterozoic amalgamation of the SFC and its margins involved a collision of two continental plates along with intervening micro-continents and magmatic arcs around 2100 Ma. Substantial parts of the colliding plates are preserved as the Archaean nuclei of the SFC in South America and Congo craton in central West Africa (Fig. 1a,b; e.g., Teixeira and Figueiredo, 1991; Ledru et al., 1994a,b; Alkmim and Marshak, 1998; Feybesse et al., 1998; Barbosa and Sabaté, 2004; Noce et al., 2007; Heilbron et al., 2010; Seixas et al., 2012, 2013; Teixeira et al., 2015; Cruz et al., 2016). The Palaeoproterozoic orogen resulting from this collision underlies the eastern and western margins of these cratons, as well as the terrain that once linked them, the São Francisco - Congo cratonic bridge (Fig. 1a,b; Porada, 1989). The cratonic bridge, which was broken apart during the opening of the South Atlantic in the Lower Cretaceous and is now exposed in eastern Brazil and Gabon, preserves a complete segment of the Palaeoproterozoic orogenic edifice. Outside the cratons, the Palaeoproterozoic orogen experienced intensive reworking during the Neoproterozoic Brasiliano/Pan-African orogenies.

The assembly of the southern São Francisco craton (SSFC) and its margins is of particular interest because it combines arc related magmatism, amphibolite to granulite facies metamorphism and closure of one of the largest and economically important Precambrian basins in

* Corresponding author.
Email address: carmenmaguilar@hotmail.com (C. Aguilar)

http://dx.doi.org/10.1016/j.precamres.2016.12.001
0301-9268/

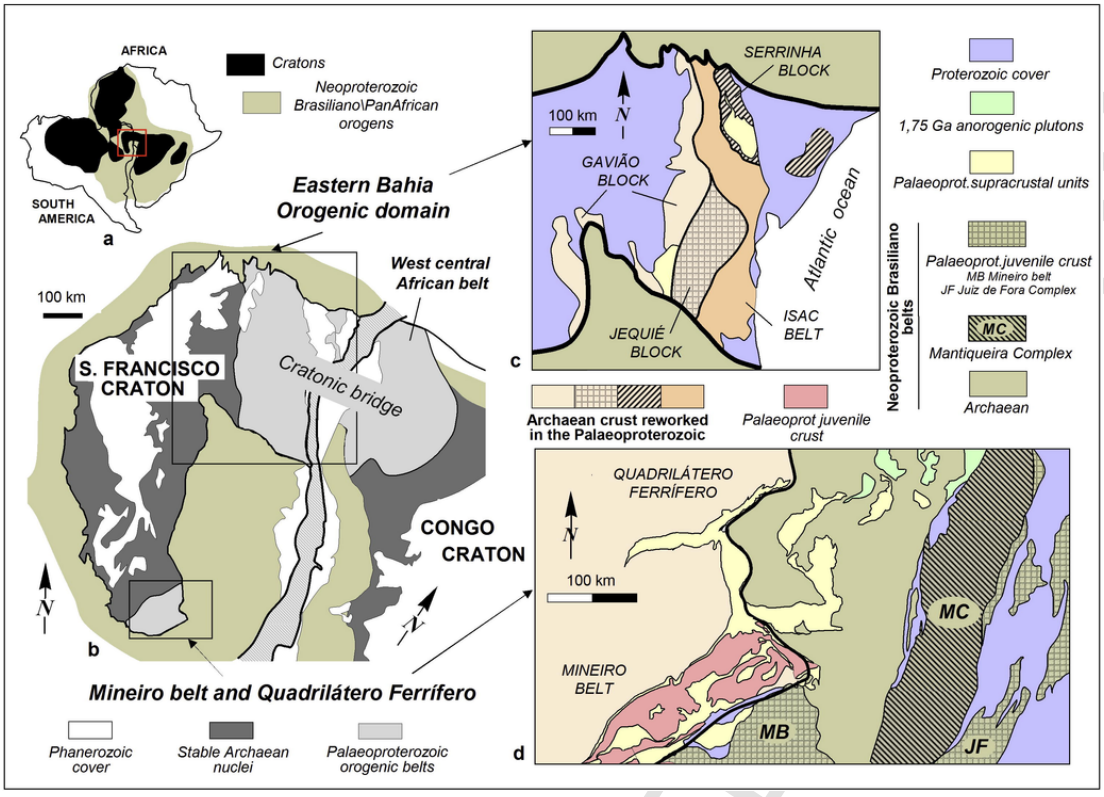

Fig. 1. Geological setting of the southern São Francisco craton and its margins. a) Cratons and Neoproterozoic orogenic belts of West Gondwana (South America and Africa); b) Preserved Archaean nuclei and Palaeoproterozoic orogenic domains of the São Francisco and Congo cratons, emphazing the crustal bridge connecting them; c) Archaean blocks of the northeastern São Francisco craton involved in the Palaeoproterozoic amalgamation of the São Francisco-Congo paleo-continent; d) Simplified tectonic map of the study area, the southern São Francisco craton (SSFC), and its eastern margin. The SSFC encompasses the western Quadrilátero Ferrífero (QF) and a substantial portion of the Minerio belt (MB). The eastern margin of the craton involved in the Neoproterozoic Araçuaí belt encompasses of the eastern QF, the southeastern Mineiro belt, as well as the Mantiqueira and Juiz de Fora complexes (Based on Barbosa and Sabaté, 2004; Noce et al., 2007; Alkmim and Martins-Neto, 2012; Teixeira et al., 2015).

South America – the Palaeoproterozoic Minas basin (e.g., Dorr, 1969; Chemale et al., 1994; Renger et al. 1995; Machado et al., 1996; Alkmim and Marshak, 1998; Hartmann et al., 2006; Noce et al.; 2007; Alkmim and Martins-Neto, 2012; Teixeira et al., 2015). Since the early investigations, this major period of tectonic activity was originally referred to as the Transamazonian event and was portrayed as a collisional episode proceeded by the development of continental and juvenile magmatic arcs. Although controversial in detail, some of these studies support a model in which closure and inversion of the Minas basin was followed by a major disturbance in the middle to upper crust at *ca.* 2095 Ma. This tectonic disturbance led to the exhumation of amphibolite-facies domes and the sinking of km-scale keels of greenschist-facies supracrustal rocks (Hippertt et al., 1992, 1994; Marshak et al., 1992; Chemale et al., 1994; Marshak et al., 1997; Alkmim and Marshak, 1998). A remaining question is if this major remobilization event represents the last thermal overprint and subsequent cooling of the Archaean nucleus of the SFC, therefore marking the final stabilization of its lithosphere.

To better understand the evolution of the São Francisco cratonic lithosphere, it is crucial to constrain the U–Pb titanite/monazite ages of the Archaean crust of the SSFC and compare them with all the available magmatic and metamorphic ages for the craton. The magmatic and metamorphic events leading to the amalgamation of the São Francisco - Congo plate have been best documented in northeastern lobe of SFC; i.e., in the Brazilian half of the cratonic bridge (Fig. 1c; e.g., Ledru et al., 1994a,b; Silva et al., 2001; Barbosa and Sabaté, 2004; Mello et al., 2006; Barbosa et al., 2008, 2012; Oliveira et al., 2010, 2011; Peucat et al., 2011; Cruz et al., 2016). Only a few data are however available for the same processes affecting the SSFC and surrounding terrains. Fig. 2 shows a number of published dates, which mark the 2100–1900 Ma Transmazonian metamorphic event in the SSFC. The low precision of these dates hinders the establishment of unifying model for the assembly and cooling of the SFC and its margins in the Palaeoproterozoic event. Consequently, the regional extent of the main Palaeoproterozoic metamorphic event across the SSFC is poorly constrained, and the causal link between the metamorphic/dome-and-keel event in the SSFC and magmatic arcs to the east (i.e., Mineiro belt and Mantiqueira Complex) requires additional studies.

In this paper, we investigate the extension of this Palaeoproterozoic thermal overprint in the Archaean – Palaeoproterozoic basement of the southern São Francisco craton and its margin using U–Pb dating of accessory titanite and monazite. These two accessory minerals are ideal U–Pb chronometers because they are sensitive to thermal overprints (Gascoyne, 1986; Parrish, 1990; Cherniak, 1993; Childe et al., 1993; Mezger et al., 1993; Hawkins and Bowring, 1997) and therefore they provide timing constraints on the thermal history of high-grade terrains. The newly acquired age data were combined with published metamorphic/magmatic ages to attempt a correlation with the crustal segments of the northern part of the São Francisco Craton

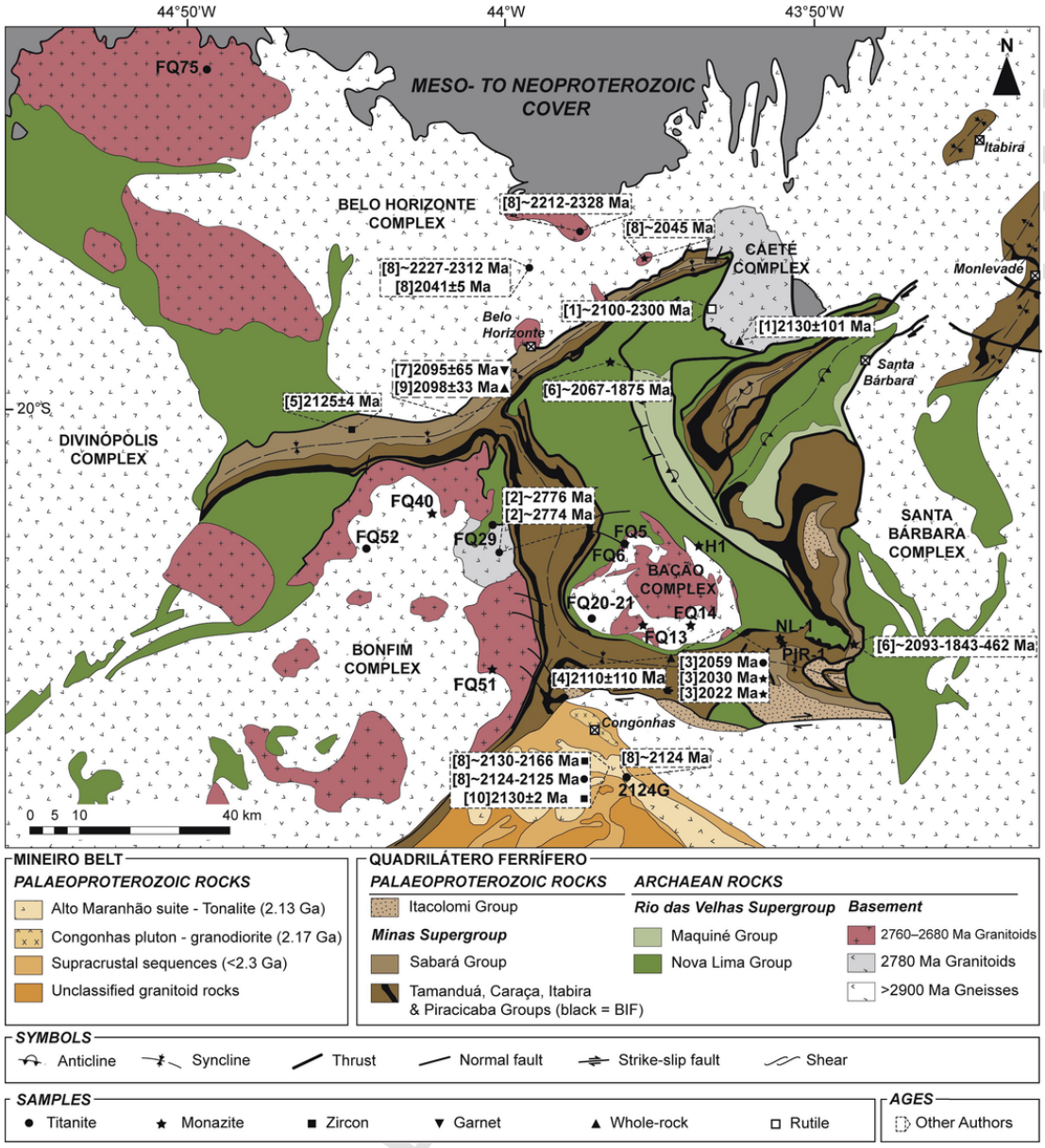

Fig. 2. Geological map of southernmost Southern São Francisco craton. The location of the samples used in this study and previously published Palaeoproterozoic metamorphic ages are plotted in the map (ages are compiled in Table 1). Reference: [1] Belo de Oliveira and Teixeira, 1990; [2] Machado and Carneiro, 1992; [3] Machado et al., 1992; [4] Babinski et al., 1995; [5] Machado et al., 1996; [6] Schrank and Machado, 1996a; Schrank and Machado, 1996b; [7] Marshak et al., 1997; [8] Noce et al., 1998; [9] Brueckner et al., 2000; and [10] Seixas et al., 2013.

and to make inferences about the timing of the consolidation of the craton.

2. The southern São Francisco craton and its margin

The São Francisco craton consists of an Archaean–Palaeoproterozoic block surrounded by Neoproterozoic belts developed during the 630–490 Ma Brasiliano/Pan-African collage of West Gondwana and is almost entirely covered by Proterozoic (<1.8 Ga) and Phanerozoic sedimentary units (Fig. 1). The craton is made up of a major N-S trending Archaean block, fringed to the northeastern and at its southern end by Palaeoproterozoic orogenic belts (Almeida et al., 1981; Teixeira et al., 2000; Barbosa and Sabaté, 2004; Alkmim and Martins-Neto, 2012). In the northeastern lobe of the craton, the Palaeoproterozoic Eastern Bahia orogenic domain comprises four distinct Archaean nuclei: the Gavião, Jequié, Itabuna-Salvador-Curaçá (ISAC) and Serrinha blocks, bounded by major *ca.* 2100 Ma old sutures zones (Fig. 1c; e.g., Teixeira and Figuereido, 1991; Barbosa and Sabaté, 2004). The southernmost sector of the craton exposes a relatively small portion of the Palaeoproterozoic orogen, which encompasses the region of the mining district known as the Quadrilátero Ferrífero and the adjacent Mineiro belt (Figs. 1d and 2). The São Francisco crust extends further east and southeast beyond the boundaries of the craton, forming the basement of the adjoining Neoproterozoic Araçuaí and Ribeira belts. In these belts, the craton crust is represented by the Mantiqueira Complex (Fig. 1d; e.g., Teixeira and Figueiredo, 1991; Alkmim and Marshak, 1998; Noce et al., 2007; Heilbron et al., 2010; Teixeira et al., 2015).

2.1. The Quadrilátero Ferrífero

The exposed section of the Quadrilátero Ferrífero consists of four principal lithostratigraphic units (see Fig. 2). The Archaean basement occurs mainly in form of km-scale domes, which include the Bonfim, Bação, Belo Horizonte, Santa Barbara, Caeté and Divinópolis complexes (Fig. 2). Due basically to lithological differences, the basement assemblages forming the various domes of the region are viewed as individual complexes and named according to their structural expressions (Machado et al., 1992; Machado and Carneiro, 1992; Noce, 1995; Teixeira et al., 2000; Lana et al., 2013; Romano et al., 2013; Farina et al., 2015a,b). These complexes are composed of several phases of (>2900 Ma) trondhjemite, tonalite and granodiorite (TTG) gneisses, showing a penetrative amphibolite-facies foliation and locally converted into stromatic migmatites (Carneiro, 1992; Noce, 1995). This foliation underwent a complex succession of folding and refolding, which testifies to the polyphase deformation history of Archaean rocks in the SSFC. The TTG gneisses are intruded by comparatively small 2780 Ma plutons, which are known as Samambaia tonalite and as Caeté trondhjemite (Fig. 2; e.g., Machado and Carneiro, 1992; Machado et al., 1992). These two magmatic phases are typically intruded by multiple younger 2760–2660 Ma granitoid suites and m- to cm-thick leucogranitic sheets sub-parallel to the gneissosity as well as crosscutting younger felsic and/or pegmatitic dikes (Lana et al., 2013; Farina et al., 2015a). These granitoids are in tectonic/fault contact with rocks of the Rio das Velhas and Minas Supergroups.

The Archaean Rio das Velhas Supergroup is Archaean greenstone belt subdivided into the Nova Lima and Maquiné Groups (Fig. 2; Dorr, 1969). The Nova Lima, which occurs at the base of the sequence, is characterized by the association between mafic and ultramafic rocks (komatiite–basalt), evolved volcanic, volcanoclastic rocks and immature clastic sediments that indicate a submarine environment for the volcanism (Ladeira, 1980; Schrank et al., 1990; Zuccheti et al., 2000a,b; Baltazar and Zuccheti, 2007). Three felsic volcanic events mark the final of deposition of the Nova Lima Group from *ca.* 2792 to 2751 Ma (Machado et al., 1992, 1996; Noce et al., 2005), whereas two sandstones from the top of the Nova Lima Group gave a maximum depositional age of 2749 ± 7 Ma (Hartmann et al., 2006). The Maquiné Group represents a 2 km-thick clastic association of conglomerates and sandstones, which comprise a flysch to molasse-type sequence. This sequence was deposited by erosion of a continental block ranging in ages from 3260 to 2877 Ma (e.g., Machado et al., 1996). However, a maximum depositional age of *ca.* 2730 Ma was proposed by Moreira et al. (2016). Gradational and discordant contacts can be observed between both groups, although fault zones often overprinted the contacts (Dorr, 1969).

The Minas Supergroup, which is divided into the Tamanduá, Caraça, Itabira, Piracicaba and Sabará Groups (Fig. 2), is a ~6 km-thick package of clastic and chemical rocks lying unconformably on the Archaean greenstone belt (Dorr, 1969; Renger et al., 1995; Machado et al., 1996; Hartmann et al., 2006). According to Alkmim and Marshak (1998), these rocks represent a passive-margin to syn-orogenic sedimentary package tracking the operation of a Wilson cycle between *ca.* 2600 and 2100 Ma. Finally, the Itacolomi Group is the youngest unit of the Palaeoproterozoic supracrustal sequence. The Group comprises an up to 2 km-thick pile of alluvial sediments that is separated from the Minas Supergroup by a regional unconformity. The Itacolomi Group is viewed as an intermontane molasse accumulated during the collapse phase of the Rhyacian orogeny (Alkmim and Martins-Neto, 2012).

2.2. The Mineiro belt and Mantiqueira Complex

The Mineiro belt consists essentially of Siderian to Rhyacian juvenile granitoids and volcanosedimentary sequences, representing a magmatic arc terrane accreted to the Archaean nucleus of the SFC at *ca*. 2100 Ma (e.g., Noce et al., 2000; Teixeira et al., 2000, 2015; Ávila et al., 2010, 2014). The most import granitoid assemblages forming the belt are: Lagoa Dourada (*ca.* 2360–2350 Ma), Serrinha-Tiradentes (*ca.* 2230–2200 Ma), Ritápolis (*ca.* 2150 Ma) and Alto Maranhão suites (*ca.* 2130–2121 Ma). These suites are made up of TTG gneisses, weakly to non-deformed plutons with sanukitoid affinity (gabbro, diorite and granite) as well as by subvolcanic and volcanic rocks. The Alto Maranhão suite, located in the northernmost part of Mineiro belt (sampled area; see Fig. 2), is composed by hornblende-bearing tonalites hosting dioritic mafic enclaves that exhibit a marked sanukitoid chemical affinity; i.e., high Mg associated to high LILE and LREE contents (Seixas et al., 2013). According to Seixas et al. (2013), the suite was produced through partial melting of a metasomatized mantle wedge above a Palaeoproterozoic subduction zone. In addition, three volcano-sedimentary sequences are tectonically associated with the Palaeoproterozoic framework (*ca.* 2230–2200 Ma; Ávila et al., 2010, 2014). These sequences crop out as elongated and discontinuous greenstone belts and are crosscut by some of Palaeoproterozoic plutons (Fig. 2). The lithological assemblage characteristic of the Mineiro belt extends further southeast beyond the SFC (Fig. 1d).

The Mantiqueira Complex is considered to be the easternmost extension of the Archean basement of the southern São Francisco craton, deeply reworked during both the Palaeo- and Neoproterozoic orogenic events recorded in the region (e.g., Teixeira, 1996, 2000; Heilbron et al., 2000; Duarte et al., 2004, 2005; Noce et al., 2007; Heilbron et al., 2010). The complex is very heterogeneous and includes several calc-alkaline gneiss–migmatitic suites with amphibolite layers, which consist predominantly of banded biotite-amphibolite orthogneisses. The whole unit was in turn intruded by alkaline felsic plutons and by younger felsic and mafic dikes approximately between *ca*. 2180 and 2040 Ma. Available Rb–Sr and U–Pb isotopic data reveal a complex and protracted evolution for the magmatic arc plutons (e.g., Fischel et al., 1998; Ragatky et al., 1999; Brueckner et al., 2000; Heilbron et al., 2001, 2010; Silva et al., 2002; Noce et al., 2007). According to these authors, the Mantiqueira Gneisses record crystallization ages from *ca*. 2203 to 2041 Ma in zircon rims and show a large amount of inherited Archaean zircon cores between *ca.* 3200 and 2600 Ma. These data together with T_{DM} model ages ranging from 3.2 to 2.9 Ga and strongly negative Epsilon Nd ($\varepsilon_{Nd}(t) = -9$ to -12) suggest that the Palaeoproterozoic rocks derived from a crust-contaminated magma at an active-margin setting (Noce et al., 2007; Heilbron et al., 2010).

The Mantiqueira Complex is bounded to the east by a major shear zone, which separates it from the Juiz de Fora Complex (Fig. 1d). Consisting essentially of granulite grade 2400–2100 Ma juvenile granitoids (enderbites and mafic rocks), the Juiz de Fora Complex is portrayed as an assemblage of intra-oceanic magmatic arc (Machado et al., 1996; Silva et al., 2002; Noce et al., 2007; Heilbron et al., 2010).

3. Proterozoic metamorphic events documented in the SSFC and Mantiqueira complex

The available metamorphic ages are scattered in studies that were mainly focused on defining the age of magmatic events. Some

geochronological data suggest that an amphibolite facies metamorphic event overprinted the Archaean orthogneisses and greenstone belt, as well as the Palaeoproterozoic supracrustal rocks in the SSFC between *ca*. 2098 and 1989 Ma (see Fig. 2 and Table 1; e.g., Belo de Oliveira and Teixeira, 1990; Machado et al., 1992, 1996; Babinski et al., 1995; Schrank and Machado, 1996a,b; Marshak et al., 1997; Noce et al., 1998; Brueckner et al., 2000; Vlach et al., 2003). In contrast, two Palaeoproterozoic metamorphic events dated between 2250 and 2050 Ma overprinted the volcano-sedimentary sequences as well as the orthogneisses and some intrusive plutons in the Mineiro belt (Cherman, 1999; Ávila, 2000; Silva et al., 2002; Toledo, 2002; Ávila et al., 2004, 2008). The first event (*ca.* 2250–2190 Ma) reached low- to medium-grade amphibolite-facies (Cherman, 1999; Toledo, 2002), whereas the second event (*ca.* 2131–2100 Ma) attained greenschist- to lower amphibolite-facies (Ávila, 2000; Ávila et al., 2004, 2008). A third and last event was mainly recognized in São Tiago gneiss, yielding a U–Pb zircon age of 2050 ± 12 Ma (Silva et al., 2002).

Finally, units of the Quadrilátero Ferrífero and Mineiro belt were locally affected by greenschist-facies metamorphism and deformation structures associated with the Neoproterozoic Brasiliano event (*ca.* 630–490 Ma) along the southeastern margin of the craton (e.g., Chemale et al., 1994; Alkmim and Marshak, 1998). In contrast, the Mantiqueira Complex was intensively deformed and metamorphosed under amphibolite conditions in the Neoproterozoic (Figueiredo and Teixeira, 1996; Silva et al., 2002; Heilbron et al., 2001, 2010; Duarte et al., 2005; Noce et al., 2007; Silva et al., 2015). A Sm–Nd garnet-whole rock isochron obtained by Brueckner et al. (2000) in the Mantiqueira Gneisses has yielded a metamorphic age of 563 ± 19 Ma.

4. U–Pb geochronological results

In order to establish a coherent sequence of metamorphic ages in the SSFC and Mantiqueira Complex, monazite and titanite grains were separated from a batch of 15 samples of the SSFC (see Fig. 2). U–Pb titanite and monazite were dated via Laser Ablation – Sector Field – Inductively Coupled Plasma Mass Spectrometry (LA-SF-ICPMS). Details of the methodology can be found in the Supplementary Material (Appendix A). The ages are summarized in Table 1 while the original data together with the samples' locations are provided in Appendix B of the Supplementary Material (Tables B1 and B2). Representative Scanning Electron Microscope – Back-Scattered Electron (SEM-BSE) images of titanite and monazite grains are shown in Fig. 3. Representative Concordia and $^{207}Pb/^{206}Pb$ weighted average age diagrams are presented in the Figs. 4 and 5.

4.1. U–Pb titanite and monazite ages in different rocks of the Archaean basement

4.1.1. Bação complex

Seven samples collected in the Archaean rocks of the Bação Complex (central Quadrilátero Ferrífero) contain titanite or monazite grains (see Fig. 2). These samples correspond to three distinct gneisses (samples FQ6, FQ13 and FQ20), a small granitic stock (sample FQ5), a leucogranitic dike intruding into the gneisses (sample FQ21) and a migmatite (sample FQ14).

Sample FQ5 is a medium to coarse-grained grey granitoid intruded into banded gneiss in the northern margin of the dome (Fig. 2). The granitoid contains monazite ranging in size from 100 to 300 μm. Monazite occurs as yellow grains with irregular shapes, biotite and zircon inclusions and covered by sugary-textured oxides. Compositional (BSE) images reveal no detectable internal zonation (Fig. 3a). A total of 35 analyses were performed on 13 grains, yielding concordant to discordant points with $^{207}Pb/^{206}Pb$ ages that range from 2590 to 2870 Ma (Table B1). These points define a Pb-loss line that intercepts the Concordia at 1105 ± 320 Ma and 2752 ± 28 Ma. The result produces a high MSWD (10) that can be considerably lowered if we consider only 6 concordant analyses to calculate the weighted mean, resulting in a mean age of 2772 ± 14 Ma with an acceptable MSWD value (1.10; Fig. 4a). This age is slightly older than the crystallization age of 2744 ± 10 Ma obtained on zircon rims by Romano et al. (2013; sample MR11).

Sample FQ6 is a fine-grained banded gneiss intruded by FQ5 and exposed a few km away from the northern border of the dome (Fig. 2). The crystallization age of this sample was obtained by U–Pb zircon analyses performed on oscillatory zoned cores, yielding an age of 2764 ± 10 Ma (Lana et al., 2013; sample D12). The orthogneiss includes scarce grains of brown titanite (up to 200 μm). In fact, only 15 grains were extracted from *ca.* 5 kg of sample. Titanite is irregular in shape and homogeneous. A total of 20 spots were analyzed on 8 grains. The $^{207}Pb/^{206}Pb$ data are spread along Concordia from 1981 to 2145 Ma (Table B2), yielding a weighted mean age of 2016 ± 8 Ma (MSWD = 0.64) for 8 concordant analyses (Fig. 5a). This age matches well with the few available Paleoproterozoic ages in the area; thus, we can interpret that this rock was affected by the Palaeoproterozoic event (Table 1).

Sample FQ13 is a spotted medium-grained gneiss collected in the southern portion of the dome (Fig. 2). Zircon from this sample gave a magmatic age at 2790 Ma and a metamorphic age at 2701 Ma (Farina et al., 2015a). The orthogneiss contains both yellow and brown monazite grains (up to 100 μm). All monazites occur as euhedral to subhedral grains with sub-spherical to lentil morphologies. Compositional (BSE) images reveal that most of the grains exhibit a complex concentric zoning, with irregular lower BSE response central regions surrounded by brighter BSE areas. In contrast, some of them show little or no variation in BSE response. LA-SF-ICPMS dating did not identify any age difference either between dark and bright areas within individual grains or between grains. A total of 20 spot analyses were carried out for each monazite type on 9 brown grains and on 7 yellow grains. Of the 40 analyses, 23 concordant ages yielded a weighted mean age of 2017 ± 7 Ma (MSWD = 1.06; Fig. 5b). The remaining 17 analyses were excluded because highly discordant. Therefore, the zircon and monazite ages suggest that the gneiss was affected by two metamorphic events: one of them at 2701 Ma (Farina et al., 2015a) and another one to 2017 Ma.

Sample FQ14 is a migmatite collected in the southeastern portion of the dome (Fig. 2). This sample, in which leucosomes and melanosomes are mixed, contains yellow monazite with a size of more than 200 μm, zircon inclusions and covered by sugar-textured oxides. Compositional (BSE) images of this yellow monazite show weak patchy zoning, with multiple zones of brighter BSE response. A total of 25 analyses were performed on 8 grains. The analyses yield concordant to discordant $^{207}Pb/^{206}Pb$ ages that range from 1887 to 2062 Ma (Table B1). The best estimate age was obtained from 14 concordant analyses, yielding a weighted mean age of 1939 ± 10 Ma (MSWD = 0.68; Fig. 5c). The remaining 11 analyses were excluded because highly discordant. This age, which is similar to the few available Palaeoproterozoic ages, suggests that the migmatite was affected by the Palaeoproterozoic metamorphic event.

Samples FQ20 and FQ21 were collected in the Serrinha quarry in the southwestern portion of the dome (Fig. 2). Sample FQ20 is a strongly banded, fine- to medium-grained gneiss that crystallized at 2918 ± 10 Ma and was metamorphosed at around 2775 Ma (Lana et

Table 1
Summary of all available Palaeoproterozoic ages and those obtained in this study for different rocks in the Southern São Francisco Craton. References: [1] Teixeira, 1985; [2] Belo de Oliveira and Teixeira, 1990; [3] Machado and Carneiro, 1992; [4] Machado et al., 1992; [5] Babinski et al., 1995; [6] Schrank and Machado, 1996a; Schrank and Machado, 1996b; [7] Teixeira et al., 1996; [8] Marshak et al., 1997; [9] Noce et al., 1998; [10] Brueckner et al., 2000; [11] Campos et al., 2003; [12] Vlach et al., 2003; [13] Seixas et al., 2013; [14] Tassinari et al., 2015.

Sample	Rock-type	Mineral or	Dating Method	*AGE (Ma)*			Reference
		rock date		Magmatic	Metamorphic	Mylonitic	
QUADRILÁTERO FERRÍFERO PROVINCE							
Archean basement							
Bação Complex							
M-88–13-D	amphibolite dike	Titanite	U–Pb TIMS		2059 ± 6		[4]
M-88–13-A	pegmatite vein	Monazite	U–Pb TIMS		*ca.* 2030		[4]
FQ5	granitoid	Monazite	U–Pb LA-ICPMS	2772 ± 14			this study
FQ6	TTG gneiss	Titanite	U–Pb LA-ICPMS		2016 ± 8		this study
FQ13	TTG gneiss	Monazite	U–Pb LA-ICPMS		2017 ± 7		this study
FQ14	migmatites	Monazite	U–Pb LA-ICPMS		1938 ± 10		this study
FQ20	TTG gneiss	Titanite	U–Pb LA-ICPMS		*ca.* 2687 – 2049		this study
FQ21	Leucogranite	Titanite	U–Pb LA-ICPMS		2080 ± 13		this study
Belo Horizonte Complex							
N-4	Córrego do Brumado granite	Monazite	U–Pb TIMS		*ca.* 2045		[9]
N-33A-1/2	migmatitic gneiss	Titanite	U–Pb TIMS		*ca.* 2227 – 2312		[9]
N-33B-5	luecosome	Titanite	U–Pb TIMS		2041 ± 5		[9]
N-57–4 to 7	Santa Luzia granite	Titanite	U–Pb TIMS		*ca.* 2212 – 2328		[9]
FQ75	amphibolite dike	Titanite	U–Pb LA-ICPMS		2066 ± 6		this study
Bonfim Complex							
625–3	Samambaia tonalite	Titanite	U–Pb TIMS	*ca.* 2776			[3]
656–4	Samambaia tonalite	Titanite	U–Pb TIMS	2774 ± 6			[3]
FQ29	Samambaia tonalite	Titanite	U–Pb LA-ICPMS		2731 ± 4		this study
FQ40	TTG gneiss	Monazite	U–Pb LA-ICPMS		1964 ± 12		this study
FQ51	granitoid	Monazite	U–Pb LA-ICPMS		2015 ± 61		this study
FQ52	TTG gneiss	Titanite	U–Pb LA-ICPMS		2042 ± 7		this study
Caeté Complex							
Ponto A	mylonitized granitoid	Whole-rock	Rb–Sr isochron			2130 ± 101	[2]
Ponto B	mylonitized granitoid	Rutile	U–Pb			*ca.* 2100 – 2300	[2]
Rio das Velhas greenstone belt							
Nova Lima Group							
M-88–15	pegmatite vein	Monazite	U–Pb TIMS		*ca.* 2022		[4]
MV-4	felsic tuff	Monazite	U–Pb ID-TIMS		*ca.* 2067 – 1875		[6]
1c,r	chl-ms-bi schist	Monazite	EPMA		*ca.* 2108 – 2086		[12]
2c,r	chl-ms-bi schist	Monazite	EPMA		*ca.* 2046 – 2024		[12]

Table 1 (*Continued*)

Sample	Rock-type	Mineral or	Dating Method	*AGE (Ma)*			Reference
		rock date		Magmatic	Metamorphic	Mylonitic	
H-1	bi-qt-chl-schist	Monazite	U–Pb LA-ICPMS		2613 ± 11		this study
NL-1	quartzitic lense	Monazite	U–Pb LA-ICPMS		2051 ± 18		this study
Turmalina mine	metasediment	garnet	Sm–Nd isochron		2148 ± 39		[14]
Turmalina mine	metasediment	WR-Bt-Ms	Rb–Sr isochron		*ca.* 2214 – 1929		[14]
Turmalina mine	metasediment	Arsenopyrite	Rb–Sr isochron		*ca.* 2180		[14]
Turmalina mine	metasediment	Biotite	K–Ar dating		2005 ± 6		[14]
Turmalina mine	metasediment	Arsenopyrite	Pb–Pb isochron		1946 ± 24		[14]
Maquiné Group							
M93-1	quartzite	Monazite	U–Pb ID-TIMS		*ca.* 2020 – 1989		[6]
Minas Supergroup							
Caraça Formation							
MGF1A	orthoquartzite	Monazite	U–Pb ID-TIMS		*ca.* 2093		[6]
Piracicaba Formation							
MF-1-A1	dolomitic marble	Whole-rock	Pb–Pb isochron		2110 ± 110		[5]
PIR-1	ferruginous metasandstone	Monazite	U–Pb LA-ICPMS		*ca.* 2173 – 546		this study
Sabará Formation							
Serra do Curral	grt-sill-ms schist	WR-Ms-Grt	Sm–Nd isochrons		2095 ± 65		[8]
GT-59	grt-sill-ms schist	WR-Ms-Grt	Sm–Nd isochrons		2098 ± 33		[10]
MINEIRO BELT							
Alto Maranhão suite							
N-22–1/2	tonalite	Zircon	U–Pb TIMS	*ca.* 2130 – 2166			[9]
N-22–3/4	tonalite	Titanite	U–Pb TIMS	*ca.* 2124 – 2125			[9]
N-18	tonalite	Titanite	U–Pb TIMS	*ca.* 2124			[9]
T15	tonalite	Zircon	U–Pb ID-TIMS	2130 ± 2			[13]
T3	tonalite	Zircon	U–Pb ID-TIMS	2128 ± 10			[13]
2124G	tonalite	Titanite	U–Pb LA-ICPMS		2065 ± 6		this study
PASSA TEMPO COMPLEX							
1	enderbite	biotite	K–Ar dating		1780 ± 54*		[11]
2	amphibolite	amphibole	K–Ar dating		2005 ± 60		[11]
2	granite	whole-rock	Rb–Sr isochron		1900 ± 108*		[11]
3	gneiss	biotite	K–Ar dating		1745 ± 52*		[11]
3a,b,c,d	gneiss	whole-rock	Rb–Sr isochron		2280 ± 220		[11]
4	gneiss	biotite	K–Ar dating		1845 ± 55*		[11]
CAMPO BELO - DIVINÓPOLIS COMPLEXES							
WT-17A	gneiss	hornblende	K–Ar dating		2161 ± 125		[1]
WT-17A1	gneiss	biotite	K–Ar dating		1996 ± 60		[1]
WT-17C	gneiss	biotite	K–Ar dating		1926 ± 58		[1]
WT-18	gneiss	biotite	K–Ar dating		2144 ± 64		[1]
WT-12B	amphibolite (melanosome)	hornblende	K–Ar dating		2077 ± 62		[1]
WT-8	gneiss	biotite	K–Ar dating		2041 ± 61		[7]
SF/WT-14A	gneiss	biotite	K–Ar dating		2036 ± 61		[1]

Table 1 (*Continued*)

Sample	Rock-type	Mineral or	Dating Method	*AGE (Ma)*			Reference
		rock date		Magmatic	Metamorphic	Mylonitic	
WT-16	gneiss	biotite	K–Ar dating		1999 ± 60		[1]
WT-7.1	gneiss	biotite	K–Ar dating		1998 ± 61		[7]
WT-14	gneiss	biotite	K–Ar dating		1954 ± 59		[1]
WT-21	gneiss	biotite	K–Ar dating		1917 ± 57		[1]
AP/WT-9ACK	gneiss	biotite	K–Ar dating		1898 ± 57*		[1]
WT-15D2	gneiss	biotite	K–Ar dating		1896 ± 60*		[1]

* cooling ages.

al., 2013; sample D07A). The banded orthogneiss contains brown titanite that varies in size from 100 to 200 μm. Titanite grains are euhedral to subhedral, generally broken and host ilmenite and zircon inclusions. Compositional (BSE) images show a more complex texture, with varied zoning patterns from simple to complex concentric or patchy, with non- to lightly luminescent parts (Fig. 3b). A total of 58 analyses were carried out on 25 grains. Individual ages range from 1842 to 2736 Ma along to the Concordia line (Table B2). They define a Pb-loss Concordia with an upper intercept of 2651 ± 44 Ma and a lower intercept of 2071 ± 29 Ma (MSWD = 0.61; Fig. 4b). Taking into account the BSE images, most of the cores or dark-colored domains yield the oldest ages, whereas data from the rims or light-colored domains are usually younger (Fig. 3b). The best estimate for the age of the cores was obtained from 3 concordant analyses, yielding a mean age of 2687 ± 9 Ma (MSWD = 0.44). This old titanite age is younger than those obtained by zircon data at *ca.* 2775 Ma (Lana et al., 2013). Regarding the rims, a reliable estimation for their age was obtained from 10 analyses, yielding a mean age of 2049 ± 6 Ma (MSWD = 1.12). The wide age spectrum is interpreted as a consequence of two distinct metamorphic histories. Sample FQ21 is a leucogranitic sheet intruded at 2774 ± 11 Ma into the banded gneiss FQ20 (Lana et al., 2013; sample D07B). The leucogranite includes brown titanite with a size of ∼200 μm. Compositional (BSE) images reveal complex concentric zoning cores surrounded by darker rims. A total of 24 spots were analyzed in the different domains of 14 grains, plotting a Pb-loss Concordia line with an upper intercept age at 2139 ± 28 Ma and a lower intercept at 1746 ± 110 Ma (MSWD = 1.12). The best estimate age was obtained from 7 concordant analyses, yielding a weighted mean age of 2080 ± 13 Ma (MSWD = 1.2; Fig. 5d). This age is consistent with the metamorphic age of the Palaeoproterozoic event, suggesting that the rock was affected by this metamorphic event (Table 1).

4.1.2. Bonfim complex

In the Bonfim Complex, located in the southwest part of the Quadrilátero Ferrífero, four samples collected from the Archaean basement contain titanite or monazite grains (see Fig. 2). These samples consist of two gneisses (samples FQ40 and FQ52) and two granitoids (samples FQ29 and FQ51).

Sample FQ29 is a medium-grained grey tonalite collected from the Samambaia pluton in the northeastern portion of the dome (Fig. 2). This sample contains brown titanite grains with a size of ∼200 μm and ilmenite inclusions. These grains are generally broken. Compositional (BSE) images reveal that brown titanite shows a zoned core surrounded by a non-luminescent rim (Fig. 3c). A total of 30 spot analyses were performed on 11 grains. The analyses produce concordant to discordant ages along the Concordia line, ranging from 2394 to 2763 Ma (Table B2). The discordant ages together with the concordant ages draw a Pb-loss line with a lower intercept at 2340 ± 180 Ma, which falls within error in the Palaeoproterozoic metamorphic ages (Fig. 4c). This fact may indicate an incomplete resetting of titanite during the Palaeoproterozoic orogen. The best estimate age is calculated from 16 analyses, yielding a mean age of 2730 ± 6 Ma (MSWD = 1.3). This age is younger than the crystallization age (∼2773–2776 Ma) obtained on titanite by Machado and Carneiro (1992) and on zircon by Farina et al. (2015a). However, it matches well with the age of the Neoarchaean metamorphic event suggested by other authors (Lana et al., 2013; Farina et al., 2015a).

Sample FQ40 is from a biotite-bearing banded gneiss crosscut by numerous foliation-parallel leucogranite sheets, collected in the northern portion of the dome (Fig. 2). U–Pb zircon data suggest that this orthogneiss crystallized at *ca.* 2850 Ma and experienced a metamorphic event at 2670 ± 15 Ma (Farina et al., 2015a). The sample includes scarce yellow monazite grains with a size of ∼100 μm and a homogeneous and luminescent zoning. A total of 20 spots were analyzed on 5 grains, yielding discordant to concordant points that define a Pb-loss line. This line intercepts the Concordia at 408 ± 920 Ma and 1980 ± 40 Ma. The result produces a high MSWD (18) that can be considerably lowered if we consider only 9 concordant analyses to calculate the weighted mean, resulting in an age of 1964 ± 12 Ma with an acceptable MSWD value (1.04; Fig. 4d). This age matches with the metamorphic age of the Palaeoproterozoic event; therefore, we can be interpreted that the rock was affected by the Paleaeoproterozoic metamorphic event (Table 1).

Sample FQ51 is a foliated light grey fine- to medium-grained granitoid from the Mamona batholith collected in the southeastern portion of the dome (Fig. 2). Zircon from this sample provides a crystallization age of 2678 Ma (Farina et al., 2015a). The sample presents yellow monazite grains with a size of ∼100–200 μm and many inclusions of zircon, and covered by sugary-textured oxides. Compositional (BSE) images show a homogenous zoning (Fig. 3d). A total of 35 analyses were carried out on 13 grains, yielding concordant to discordant points. These points define a Pb-loss line with an upper intercept age of 2002 ± 29 Ma and a lower intercept at 484 ± 150 Ma (MSWD = 1.7). A weighted mean age was estimated from 4 spot analysis, yielding a mean age of 2015 ± 61 Ma with MSWD = 4.4 (Fig. 5e) that corresponds to the Palaeoproterozoic metamorphic event (Table 1).

Sample FQ52 is a banded gneiss collected in the northwestern portion of the dome (Fig. 2). Zircon data yield a crystallization age of 2727 ± 11 Ma (Farina et al., 2015a). The sample contains brown titanite grains with a size of ∼200 μm and biotite inclusions. Compositional (BSE) images reveal that most of grains show variable BSE response with different non- to lightly luminescent parts. Others exhibit no variation in BSE response. A total of 35 spot analyses were performed on 11 grains, yielding $^{207}Pb/^{206}Pb$ ages that range from 1941 to 2152 Ma (Table B2). The best estimate age was calculated

Table 2
Summary of available Palaeoproterozoic ages in the northern part of São Francisco Craton. References: [1] Wilson, 1987; [2] Conceição, 1990; [3] Marinho, 1991; [4] Silva, 1992; [5] Vasconcelos and Becker, 1992; [6] Cheilletz et al., 1993; [7] Ledru et al., 1994a; Ledru et al., 1994b; [8] Nutman et al., 1994; [9] Sabaté et al., 1994; [10] Oliveira and Lafon, 1995; [11] Bastos Leal et al., 1996; [12] D'el-Rey Silva et al., 1996; [13] Mougeot, 1996; [14] Rosa et al., 1996; [15] Santos Pinto, 1996; [16] Silva et al., 1996; [17] Chauvet et al., 1997; [18] Ledru et al., 1997; [19] Silva et al., 1997; [20] Bastos Leal, 1998; [21] Leahly et al., 1998; [22] Oliveira et al., 1998; [23] Conceição et al., 1999; [24] Barbosa et al., 2000a; Barbosa et al., 2000b; Barbosa et al., 2000c; [25] Correa Gomes, 2000; [26] Rios et al., 2000; [27] Rosa et al., 2000; [28] Teixeira et al., 2000; [29] Silva et al., 2001; [30] Barbosa and Sabaté, 2002; [31] Conceição et al., 2002; [32] Rios, 2002; [33] Silva et al., 2002; [34] Oliveira et al., 2002a; Oliveira et al., 2002b; [35] Carvalho and Oliveira, 2003; [36] Barbosa et al., 2004; [37] Oliveira et al., 2004a; Oliveira et al., 2004b; [38] Cruz Filho et al., 2005; [39] Mello et al., 2006; [40] D'el-Rey Silva et al., 2007; [41] Rios et al., 2007; [42] Barbosa et al., 2008; [43] Costa, 2008; [44] Rios et al., 2008; [45] Leite et al., 2009; [46] Oliveira et al., 2010; [47] Silva et al., 2015; [48] Cruz et al., 2016.

Domains	Rock-type	Mineral or rock date	Dating Method	*AGE (Ma)*			Reference
				Sedimentation	Magmatic	Metamorphic	
GAVIÃO DOMAIN							
Jacobina Group							
	Serra do Corrego quartzites	detrital zircon	U–Pb	2086 ± 43			[13]
	Campo Forroso granite	Whole-rock	Rb–Sr isochron		1969 ± 29		[13]
Saúde Complex							
	paragneiss	monazite	U–Th–Pb EPMA			*ca*. 2080–2050	[45]
Mairi Complex							
	quartz-monzanite	Zircon	U–Pb SHRIMP		2126 ± 19		[19]
Contendas–Mirante greenstone belt							
	detricit sediment	Zircon	U–Pb SHRIMP	2168 ± 18			[8]
	leucosome metapelite	Whole-rock	Rb–Sr isochron		*ca*. 2000		[28]
	Calculé granite granite	Zircon	Pb–Pb singles		2015 ± 27		[15]
	Serra da Franga granite	Zircon	Pb–Pb singles		2039 ± 11		[15]
	Umburanas granite	Zircon	Pb–Pb singles		2049 ± 5		[15]
	Gameleira granite	Whole-rock	Rb–Sr isochron		1947 ± 57		[3]
Urandí-Paratinga belt							
	Guanambí-Urandí batholit	Zircon	Pb–Pb singles		*ca*. 2000–2060		[14]
	Guanambí-Urandí batholit	Whole-rock	Rb–Sr isochron		*ca*. 2000–2061		[11]; [21]
	Guanambí multiple intrusion	Zircon	U–Pb TIMS		2054 ± 8/6		[27]
		Zircon	Pb evaporation		2046 ± 10		[27]
	Cara Suja	Zircon	U–Pb TIMS		2053 ± 3		[27]
	Cerafma	Zircon	U–Pb TIMS		2050.4 ± 1.4		[27]
		Zircon	Pb evaporation		2049 ± 2		[27]
	Estreito	Zircon	U–Pb TIMS		2054 ± 3		[27]
		Zircon	Pb evaporation		2041 ± 2		[27]
Calculé Complex							
	Jussiape II granitoid	Zircon	U–Pb LA-ICPMS		2052 ± 43		[48]
	Lagoa das Almas granitoid	Zircon	U–Pb LA-ICPMS		2114 ± 24		[48]
	Humaitá granitoid	Zircon	U–Pb LA-ICPMS		2140 ± 9		[48]
	Belo Campo granitoid	Zircon	U–Pb LA-ICPMS		2049 ± 23		[48]
	Broco granitoid	Zircon	U–Pb LA-ICPMS		2039 ± 8		[48]
JEQUIÉ DOMAIN							
	Brejões charnockite	Zircon	Pb–Pb singles		2026 ± 4		[30]
	Brejões charnockite	Monazite	Pb–Pb isochron			2052 ± 2	[36]
	Brejões migmatites	Monazite	Pb–Pb TIMS			2045 ± 2.5	[36]
	Cravolândia charnockite	Monazite	Pb–Pb TIMS			2026 ± 1	[36]
	Ubaíra Enclaves granulite	Monazite	Ion Microprobe			*ca*.1965–1931	[24]

Table 2 (*Continued*)

Domains	Rock-type	Mineral or rock date	Dating Method	*AGE (Ma)*			Reference
				Sedimentation	Magmatic	Metamorphic	
	Ubaíra Enclaves granulite	Zircon	Pb–Pb singles			*ca.* 2047	[24]
	Maracás granite	Zircon	Pb–Pb singles			*ca.* 2100	[24]
	Maracás granite	Monazite	Ion Microprobe			2057 ± 7	[24]
	Jequié charnockite	Zircon	U–Pb SHRIMP		2473 ± 5	2061 ± 6	[33]
	Jequié migmatite	Whole-rock	Rb–Sr isochron			2085 ± 222	[1]
	Jequié migmatite	Whole-rock	Pb–Pb isochron			1970 ± 136	[1]
ITABUNA-SALVADOR-CURAÇA DOMAIN							
Caraíba Complex							
	Caraíba norite	Zircon	U–Pb		*ca.* 2051		[10]
	Caraíba orebody	monazite	U–Pb		2051 ± 16		[12]
	orthogneiss	Zircon	Pb–Pb		*ca.* 2100		[9]
	tonalitic orthogneiss	Zircon	Pb–Pb singles		2074 ± 9		[18]
	tonalitic orthogneiss	Zircon	U–Pb SHRIMP		2574 ± 6	2074 ± 14	[46]
	Airport G3 granite	Zircon	U–Pb SHRIMP		2027 ± 16		[46]
	Airport tonalitic orthogneiss	Zircon	U–Pb TIMS		2248 ± 36		[12]
	Airport amphibolite	Zircon	U–Pb TIMS		2577 ± 110	2082 ± 4	[40]
	Itiúba syenite	Whole-rock	Rb–Sr isochron		*ca.* 2140		[2]
	Itiúba syenite	Zircon	U–Pb SHRIMP		2084 ± 9		[37]
	Bravo granite	Zircon	U–Pb SHRIMP		*ca.* 2060		[42]
	Capela qtz-monzonite	Zircon	U–Pb SHRIMP		2078 ± 6		[46]
	Medrado gabbro	Zircon	U–Pb		*ca.* 2059		[10]
	Santanápolis syenite	Whole-rock	Rb–Sr isochron		*ca.* 2060		[2]
		Zircon	U–Pb		*ca.* 2100		[23]
	Trecho Velho serpentinites	phogopite	Ar–Ar dating			1951 ± 8*	[6]
	Braulia pegamtite	phogopite	Ar–Ar dating			1934 ± 8*	[6]
San José de Jacuípe Complex							
	granulite-facie orthogneiss	Zircon			*ca.* 2695–2634	*ca.* 2072	[19]
	leucogabbro	Zircon	U–Pb SHRIMP		2583 ± 8	2082 ± 17	[46]
Tanque Novo - Ipirá Complex							
	paragneiss	monazite	U–Th–Pb EPMA			*ca.* 2080–2050	[45]
Itabuna Complex							
	Barra do Rocha tonalite	Zircon	Pb–Pb singles		2092 ± 13		[7]
	Itabuna tonalite	Whole-rock	Pb–Pb isochron		*ca.* 2130		[30]
	Pau Brasil tonalite	Zircon	Pb–Pb singles		2089 ± 4		[25]
	Al-Mg granulite	Monazite	Ion Micropobe			*ca.* 1996–1955	[24]
	Mirabela body	Whole-rock	Sm–Nd *T*DM		*ca.* 2200		[16]
SERRINHA DOMAIN							
Caldeirão shear belt							
	quartzite	Zircon	U–Pb SHRIMP			2076 ± 10	[34]; [39]
	mafic dike	titanite	U-Pb			2039 ± 2	[34]
Rio Capim greenstone belt							
	felsic volcanic rock	Whole-rock	Pb–Pb isochron	2153 ± 79			[22]
	leucogabbro	Zircon	U–Pb TIMS		*ca.* 2138		[22]
	diorite	Zircon	U–Pb TIMS		*ca.* 2126		[22]
	metadacite	Zircon	U–Pb SHRIMP		2148 ± 9		[46]
Rio Itapicuru greenstone belt							
	basic volcanic rock	Whole-rock	Pb–Pb isochron	2209 ± 60			[4]; [29]
	basic volcanic rock	Whole-rock	Sm–Nd *T*DM	*ca.* 2200			[4]
	felsic volcanic rock	Whole-rock	Pb–Pb isochron	2109 ± 80			[4]
	felsic volcanic rock	Whole-rock	Rb–Sr isochron	2080 ± 90			[4]
	felsic volcanic rock	Whole-rock	Sm–Nd *T*DM	*ca.* 2100			[4]

Table 2 (*Continued*)

Domains	Rock-type	Mineral or rock date	Dating Method	*AGE (Ma)*			Reference
				Sedimentation	Magmatic	Metamorphic	
	andesite - dacite	Whole-rock	Pb–Pb isochron		2170 ± 60		[29]
	massive metabasalt	zircon	U–Pb SHRIMP		2145 ± 8		[46]
	porphyritic metabasalt	zircon	U–Pb SHRIMP		2142 ± 6		[46]
	dacite	zircon	U–Pb SHRIMP		2081 ± 9		[46]
	Nordestina trondhjemite	Monozircon	Pb–Pb isochron		2155 ± 9		[38]
	Eficeas granodiorite	zircon	U-Pb		2163 ± 5		[32]
	Trilhado granodiorite	zircon	U-Pb		2155 ± 9		[38]
	Trilhado granodiorite	monazite	U-Pb		2152 ± 6		[38]
	Barrocas granodiorite	Monozircon	Pb–Pb isochron		2130 ± 7		[17]
	Teofilânia granodiorite	Monozircon	Pb–Pb isochron		2127 ± 5		[39]
	Morro do Afonso syenite	zircon	U-Pb		2111 ± 10 2106 ± 6		[41]
	Itareru tonalite	zircon	U-Pb				[35]
	Fazenda Gavião granodiorite	zircon	U-Pb				[43]
	cansanção monzonite	zircon	U-Pb				[32]
	Serra do Pintado syenite		Pb–Pb isochron		2098 ± 2 2086 ± 2		[31]
	Agulhas syneite		U-Pb				[31]
	Bananas syenite						[31]
	Ambrósio granite	Zircon	U–Pb SHRIMP		2076 ± 10		[32]
	Ambrósio granite		Sm–Nd *T*DM		*ca.* 2100		[32]
	Ambrósio granodiorite	xenotime	U–Pb SHRIMP		2080 ± 2		[39]
	Poço Grande granite	Zircon	U–Pb		2070 ± 47		[20]
	Morro do Lopes granite	Zircon	U-Pb		2072 ± 1		[26]
	shear zone	biotite	Ar–Ar dating		ca. 2054–2049		[5]; [39]
	Quijingue pluton				2155 ± 8		[44]
PORTEIRINHA DOMAIN							
Córrego Tingui granitic complex							
	peraluminous leucogranite	Zircon	U–Pb SHRIMP II		2140 ± 14		[47]
Paciência alkaline suite							
	Serra Blanca foliated syenite	Zircon	U–Pb SHRIMP II		2039 ± 8		[47]

* cooling age.

from 9 analyses, yielding a concordant age of 2040 ± 7 Ma with MSWD = 1.5 (Fig. 5f).

4.1.3. Belo Horizonte Complex

In the Belo Horizonte Complex, located in the northwest part of the Quadrilátero Ferrífero, sample FQ75 collected in the northwestern portion of the dome (Fig. 2) is an amphibolite dike intruded in the Pequi pluton, which contains both yellow and brown titanite grains. All titanites are euhedral to subhedral grains with a size from 100 to 300 μm and zircon inclusions. Compositional (BSE) images show a complex concentric zoning in both grains, with irregular lower BSE response cores surround by brighter BSE regions (Fig. 3e). However, some of them exhibit a non-luminescent rim surrounding the complex concentric zoning. A total of 41 spots were analyzed on 13 brown grains, whereas 34 analyses were performed on 14 yellow grains. Taking into account both grains types and the different zones, LA-SF-ICPMS dating did not identify any significant age difference. The best estimate was obtained from 27 analysis yielding a Concordia age of 2066 ± 6 Ma with MSWD = 0.24, interpreted as the Palaeoproterozoic metamorphic age (Fig. 4e).

4.2. U–Pb monazite ages of the Archaean Rio das Velhas greenstone belt

In the central part of the Quadrilátero Ferrífero, two samples from the Rio das Velhas greenstone belt contain monazite grains (samples H1 and NL-1; see Fig. 2). Sample H1 is a biotite–quartz–chlorite schist located a few meter from the contact with the Bação Complex. Sample NL-1 is a quartzitic lens interlayered in Nova Lima mica-schist close to the contact with the Minas Supergroup in the Dom Bosco syncline.

Sample H1 contains yellow monazite grains with a size from 100 to 250 μm and a homogenous zoning (Fig. 3f). A total of 21 spot analyses were carried out on 8 grains. The obtained data yielded concordant to discordant results that define a Pb-loss line with an upper intercept age of 2617 ± 9 Ma and a lower intercept at 721 ± 230 Ma (MSWD = 1.4; Fig. 4f). These ages suggest that the monazite was crystallized during a metamorphic event at 2617 Ma and partially reset by another during another younger episode probably associated to Brasiliano orogen.

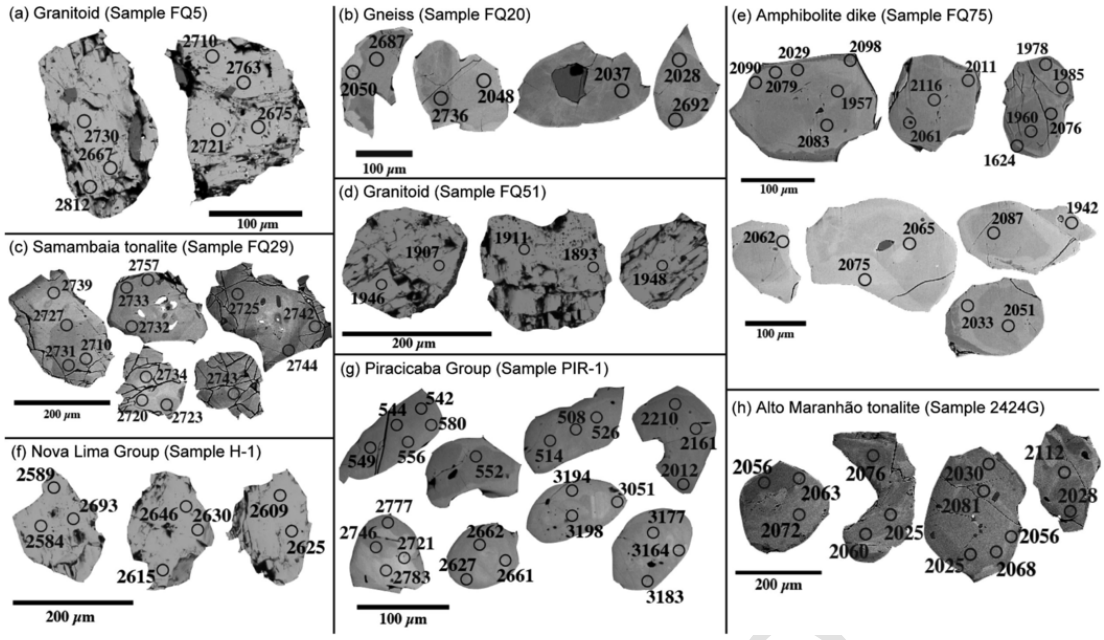

Fig. 3. Representative BSE-SEM images of the analyzed titanite and monazite with the location of the LA-SF-ICPMS spots and the measured $^{207}Pb/^{206}Pb$ ages.

Sample NL-1 contains scarce yellow monazite grains with a size of ~100 μm and a homogenous zoning. A total of 20 analyses were performed on 7 grains, yielding concordant to discordant points $^{207}Pb/^{206}Pb$ ages that range from 1705 to 2166 Ma (Table B1). These points define a Pb-loss line with an upper intercept age of 2051 ± 34 Ma and a lower intercept at 516 ± 560 Ma (MSWD = 5.0). The obtained data yielded a weighted mean age of 2051 ± 18 Ma with an MSWD of 0.99 for 14 concordant analyses (Fig. 5g). These ages indicate that the monazite was crystallized during a Palaeoproterozoic metamorphic event at *ca.* 2051 Ma, and then was partially reset probably during the Brasiliano orogeny, as suggested by the lower interception of the Pb-loss line.

4.3. U–Pb monazite ages of a metasedimentary rock of the Palaeoproterozoic Minas Supergroup

In the southeastern part of the Quadrilátero Ferrífero, sample PIR-1 from the Piracicaba Group (Minas Supergroup) located in the Dom Bosco syncline includes monazite grains (see Fig. 2). This sample is a ferruginous metasandstone interlayered in cm-levels of phyllite. It contains scarce monazite with a size of ~100 μm. Monazite occurs as euhedral to subhedral grains. Compositional (BSE) images reveal that most of the monazite grains show a weakly complex concentric zoning, whereas some of them exhibit a homogeneous zoning (Fig. 3g). A total of 40 spots were analyzed on 12 grains, yielding $^{207}Pb/^{206}Pb$ ages that range from 508 to 3198 Ma (Table B1). Taking into account the BSE images of the grains, most of the heterogeneous grains yield the oldest ages, whereas data from the homogeneous grains are usually younger. On the heterogeneous grains, fourteen concordant analyses yield a mean age of 2657 ± 9 Ma (MSWD = 0.85). For the homogeneous grains, two concordant analyses provide an age at 2173 ± 58 Ma (MSWD = 0.51) and four concordant analyses yield another one at 546 ± 3 Ma (MSWD = 1.08; Table 1). Therefore, four population ages can be registered in this sample. The older gains are interpreted as detrital monazite, owing to the Piracicaba Group must be younger than the upper Itabira Group deposited at *ca.* 2420 Ma (Babinski et al., 1995), whereas the two younger ages can correspond to two distinct metamorphic ages: the Palaeoproterozoic and Brasiliano metamorphic events.

4.4. U–Pb titanite ages of a tonalite of the Alto Maranhão suite from the Mineiro belt

In the northernmost part of the Mineiro belt, sample 2124G was taken in the Alto Maranhão pluton (Fig. 2). This sample corresponds to the one collected by Seixas et al. (2013), who obtained a titanite crystallization age of 2128 ± 10 Ma, which is consistent with the zircon and titanite data obtained by Noce et al. (1998). Sample 2124G is a tonalite that include both brown and yellow-green titanite grains. They are euhedral to subhedral grains with a size of ~100–200 μm, generally broken. Compositional (BSE) images show a complex concentric zoning with non- to lightly luminescent parts (Fig. 3h). A total of 29 spots were analyzed on 7 grains, yielding $^{207}Pb/^{206}Pb$ ages that range from 1993 to 2112 Ma (Table B2). Of the 29 analyses, 11 concordant analyses provide a mean age of 2064 ± 6 Ma (MSWD = 0.38; Fig. 4h). This age is younger than those obtained on zircon and titanite by Noce et al. (1998) and Seixas et al. (2013) and similar within error to the metamorphic age obtained for the São Thiago gneiss (2050 ± 12 Ma; Silva et al., 2002). Therefore, this fact suggests that the Alto-Maranhão tonalite was affected by a metamorphic event associated to the Palaeoproterozoic collision. The results obtained on yellow-green titanite were excluded due to the fact that it incorporates lower U concentrations in the structure (e.g., Verts and Chamberlain, 1996).

5. Discussion

5.1. Timing of the Palaeoproterozoic metamorphic event

The results obtained suggest that titanite and monazite underwent a complex history of new growth, recrystallization (dissolution/precipitation) and/or partial lead-loss to isotopic resetting during the Palaeoproterozoic metamorphic event. In some samples distinct age populations are clearly identified, whereas in other cases the data ex-

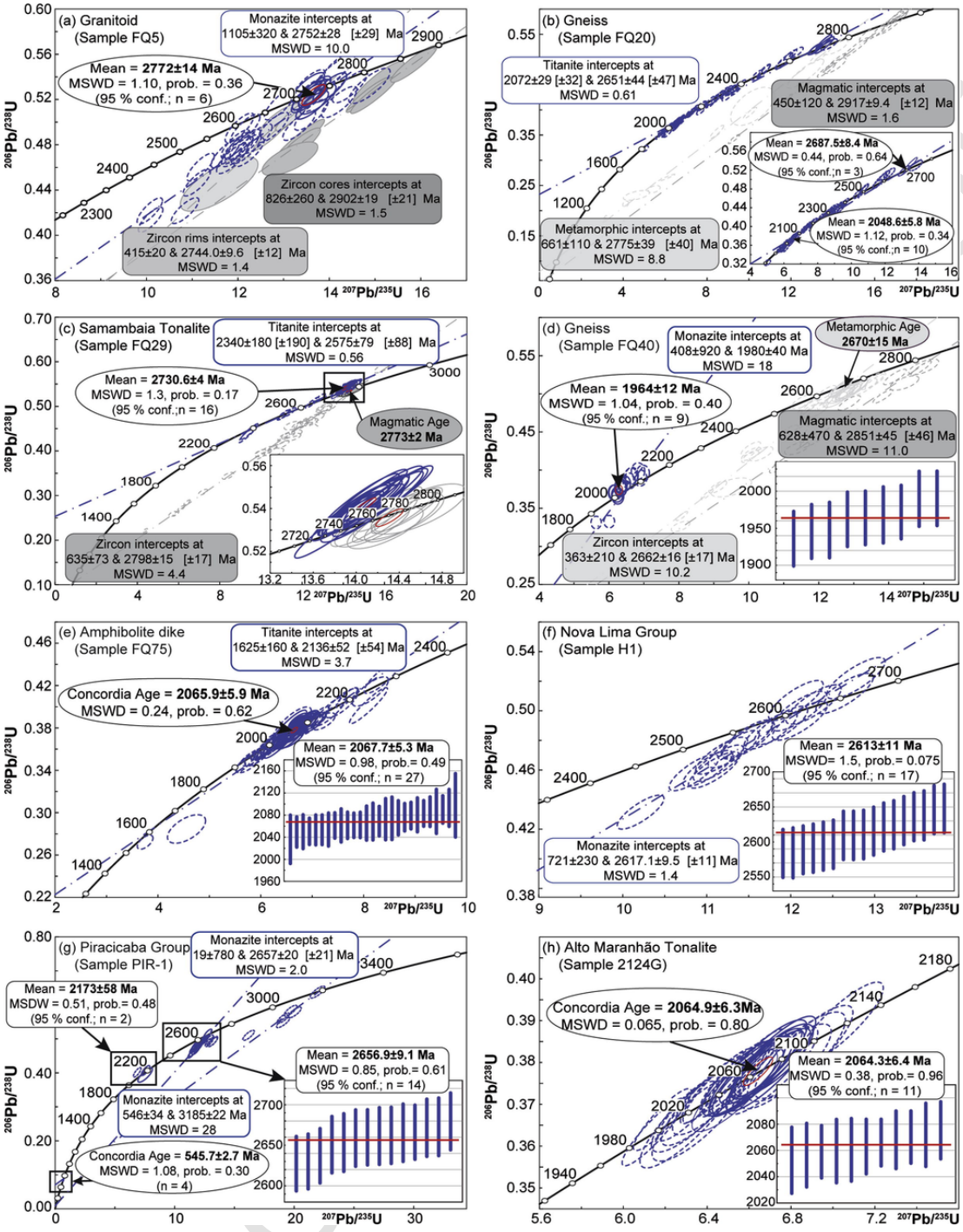

Fig. 4. Representative Concordia diagrams of LA-SF-ICPMS U–Pb titanite and monazite ages for different rocks: (a–d) gneisses and granitoids from the Bação and Bonfim complexes; (e) amphibolite dike from Belo Horizonte Complex; (f) Nova Lima Group from Rio das Velhas Supergroup; (g) Piracicaba Group from Minas Supergroup; and (h) Alto Maranhão tonalite from Mineiro Belt. The dashed ellipses represent the discordant data. The insets are either $^{207}Pb/^{206}Pb$ weighted average age plots or detailed Concordia age plots. The zircon data obtained for these samples by Lana et al. (2013), Romano et al. (2013) and Farina et al. (2015a) are outlined by grey ellipses. Error ellipses and error bars are at 2σ.

hibit a wide variation in ages that probably represent partial recrystallization and isotopic resetting. We observed that early titanite and monazite growth were preserved, yielding dates that correspond to the magmatic ages of the rock (2772 ± 14 Ma; Fig. 4a) or metamorphic events that followed magmatic crystallization (2731 ± 4 Ma and 2613 ± 11 Ma; Fig. 4c and f, respectively). Brown titanite with dark and light zones observed in an orthogneiss from the southwestern part of the Bação Complex (sample FQ20; Fig. 3b) records two different age populations, reflecting a period of growth at around 2687 Ma followed by recrystallization and/or partially resetting at around

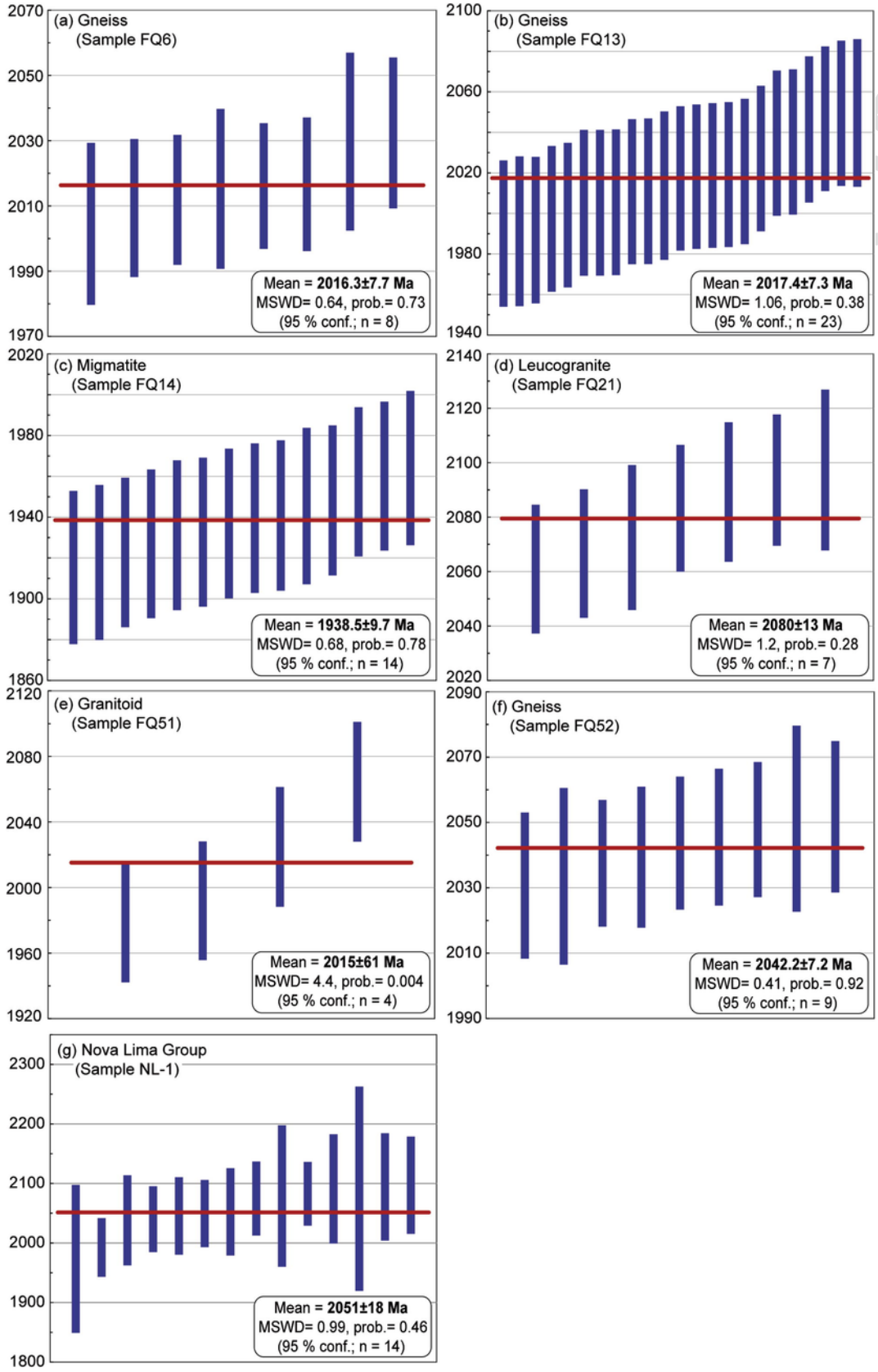
(a) Gneiss
(Sample FQ6)
Mean = 2016.3±7.7 Ma
MSWD= 0.64, prob.= 0.73
(95 % conf.; n = 8)
(b) Gneiss
(Sample FQ13)
Mean = 2017.4±7.3 Ma
MSWD= 1.06, prob.= 0.38
(95 % conf.; n = 23)
(c) Migmatite
(Sample FQ14)
Mean = 1938.5±9.7 Ma
MSWD= 0.68, prob.= 0.78
(95 % conf.; n = 14)
(d) Leucogranite
(Sample FQ21)
Mean = 2080±13 Ma
MSWD= 1.2, prob.= 0.28
(95 % conf.; n = 7)
(e) Granitoid
(Sample FQ51)
Mean = 2015±61 Ma
MSWD= 4.4, prob.= 0.004
(95 % conf.; n = 4)
(f) Gneiss
(Sample FQ52)
Mean = 2042.2±7.2 Ma
MSWD= 0.41, prob.= 0.92
(95 % conf.; n = 9)
(g) Nova Lima Group
(Sample NL-1)
Mean = 2051±18 Ma
MSWD= 0.99, prob.= 0.46
(95 % conf.; n = 14)

Fig. 5. Representative $^{207}Pb/^{206}Pb$ weighted average age plots of LA-SF-ICPMS U–Pb titanite and monazite ages for gneisses, migmatite and leucogranite from the Bação Complex (a–d), granitoid and gneiss from the Bonfim Complex (e–f) and Nova Lima Group from the Rio das Velhas Supergroup (g). Error bars are at 2σ.

2048 Ma (Fig. 4b). Therefore, the Neoarchaean ages suggest that titanite growth took place during magmatism at *ca*. 2772 Ma (Fig. 4a) or during metamorphism between *ca.* 2731 and 2613 Ma (see Table 1 and Fig 4b–c,f). Combining this data with previous U–Pb zircon data, the oldest metamorphic ages match well with the Neoarchaean age of the amphibolite-facies metamorphism between 2794 and 2760 Ma observed on many magmatic zircons overgrown by rims (e.g., Machado and Carneiro, 1992; Lana et al., 2013; Farina et al., 2015a). The youngest ages (i.e., 2687–2613 Ma) are well correlated with the metamorphic ages documented by zircon rims, especially in Passa Tempo Complex (2622–2599 Ma; Campos et al., 2003) and in Bonfim and Belo Horizonte complexes (2679–2644 Ma; Farina et al., 2015a), and with the age of small scattered granitic stocks intruding the Bonfim and Belo Horizonte complexes between 2630 and 2610 Ma (e.g., Romano et al., 2013).

Subsequent metamorphism and intrusion-related heat/fluid flow events during the Palaeoproterozoic orogeny in the SSFC (discussed below) resulted in the regional-scale recrystallization and isotopic resetting of the pre-existing titanite and monazite. Detailed compilation of the Palaeoproterozoic metamorphic ages recorded by titanite and monazite and relative ages recorded in zircon is shown in Fig. 6. The vast majority of the titanite and monazite dated in the SSFC record the thermal overprint at around 2080 and 1940 Ma, whereas zircon only records Archaean magmatic and metamorphic ages (Figs. 6 and 7). This implies that temperatures associated with closure of the Minas Basin and dome exhumation were not sufficiently high to over-

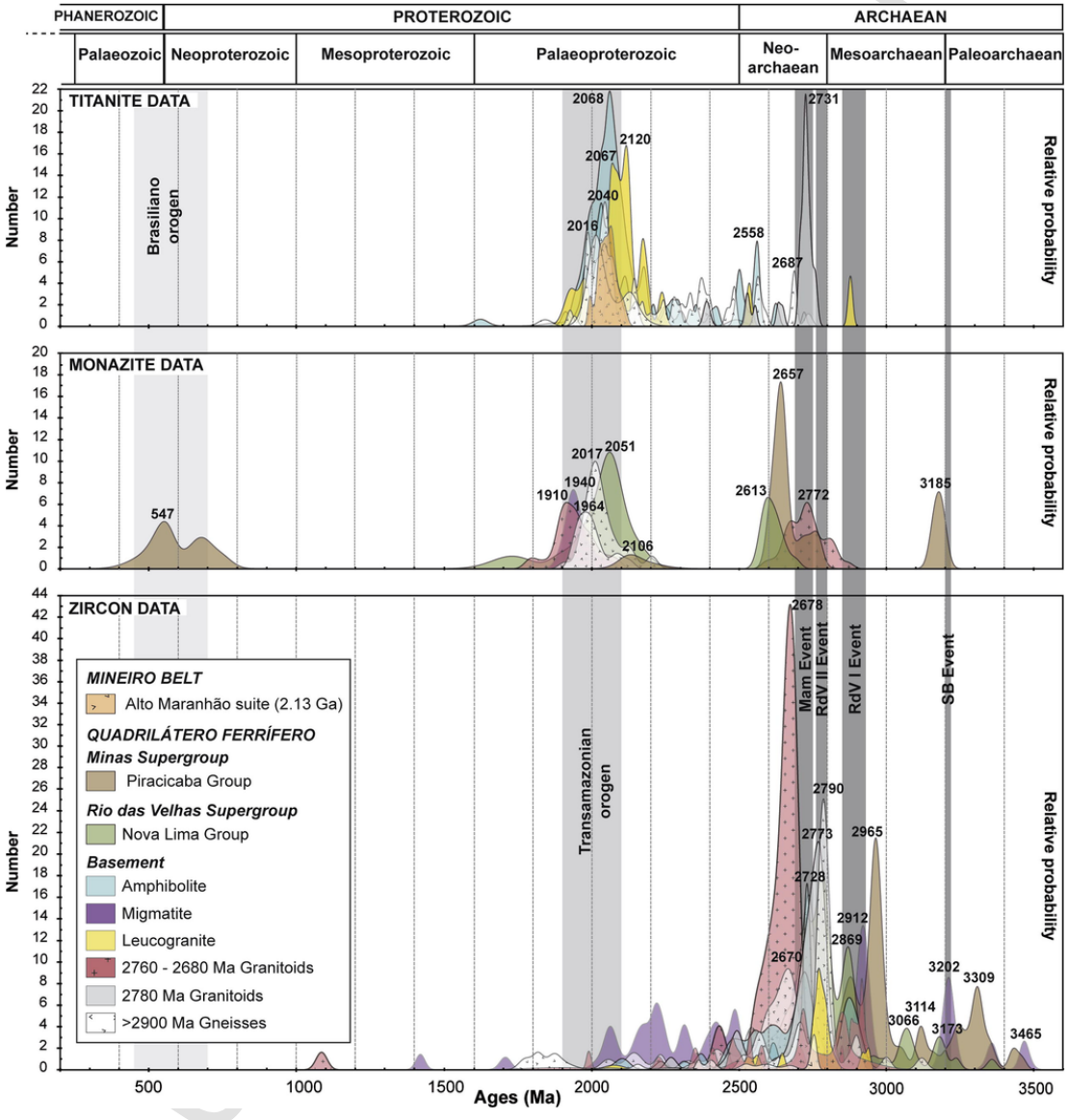

Fig. 6. Relative probability plots of U–Pb titanite and monazite ages obtained in this study and U–Pb zircon data obtained by Lana et al. (2013), Romano et al. (2013) and Farina et al. (2015a). For comparison, the age distributions of different orogens and Archean events are marked by grey-shaded areas. SB: Santa Barbara Event, RdV I and II: Rio da Velhas I and II Events, and Mam: Mamona Event.

print zircons, which can overgrow at high T conditions with melt/fluid present permitting accurate dating of high-grade metamorphism (⩾700 °C; e.g., Vavra et al., 1996; Williams et al., 1996; Lee et al., 1997; Vavra and Schaltegger, 1999; Cherniak and Watson, 2001; Rubatto et al., 2001; Williams, 2001; Hermann and Rubatto, 2003). Given the preservation of some inherited radiogenic Pb in the titanite and monazite, we can infer that the Palaeoproterozoic metamorphism reached a maximum temperature between 650 °C and 700 °C, which were proposed as the minimum closure temperature of titanite (Scott and St-Onge, 1995). This amphibolite-facies condition is in agreement with the conditions obtained by Jordt-Evangelista et al. (1992) and Cutts et al. (subm.).

5.2. *Heating and cooling of the southern São Francisco craton*

The regional extent of the Palaeoproterozoic ages we obtained in the SSFC and the surrounding terrains is shown in Fig. 7. The data also include ages for contact metamorphic rocks determined by Sm–Nd data on whole-rock, muscovite and garnets in the Palaeoproterozoic Minas Supergroup (e.g., Marshak et al., 1997; Brueckner et al., 2000). Both titanite and monazite ages overlap well with previous U–Pb SHRIMP/TIMS data for gneiss samples in the Mineiro belt and the Mantiqueira Complex (e.g., Silva et al., 2002; Noce et al., 2000; Heilbron et al., 2001; Noce et al., 2007; Heilbron et al., 2010; Seixas et al., 2012, 2013).

The Mineiro Belt records a protracted history of subduction-related magmatism in intra-ocenic settings, which started around 2470 Ma and ends around 2100 Ma (Ávila et al., 2010, 2014; Seixas et al., 2012, 2013; Barbosa et al., 2015; Teixeira et al., 2015). In marked contrast with the adjacent crustal segments, its supracrustal assemblages witnessed three metamorphic episodes dated between 2250 and 2050 Ma (Cherman, 1999; Ávila, 2000; Silva et al., 2002; Toledo, 2002; Ávila et al., 2004, 2008).

According to the available data, the emplacement of subduction-related rocks into the Archaean São Francisco craton crust (represented by the Mantiqueira Complex) started at *ca*. 2200 Ma and also ends around 2100 Ma (Noce et al., 2007; Heilbron et al., 2010), indicating that abortion of subduction as a consequence of collision with other terranes and ultimately with the Congo craton nucleus occurred at *ca*. 2100 Ma or immediately after (Fig. 8). The obtained U–Pb titanite/monazite ages seem to reflect first the syn-collisional and regionally extensive amphibolite-facies metamorphism affecting SSFC, whose climax was probably reached at *ca*. 2080 Ma (Fig. 6).

Some models proposed for the tectonic evolution of the Quadrilátero Ferrífero invocated post-orogenic extension as an effective mechanism for the development of the dome-and-keel architecture that characterizes this province (Marshak et al., 1992; Alkmim and Marshak, 1998). However, in these models subduction was supposed to be east-directed, due to the fact that the continental arc nature of the Mantiqueira Complex was not known at the time. Post-orgenic extension acting upon a back-arc region during tectonic collapse seems to be even more effective in raising the geotherms and providing heat for the subsequent generation of the dome-and-keel geometry (Fig. 8d). Published structural analyses and recent meta-

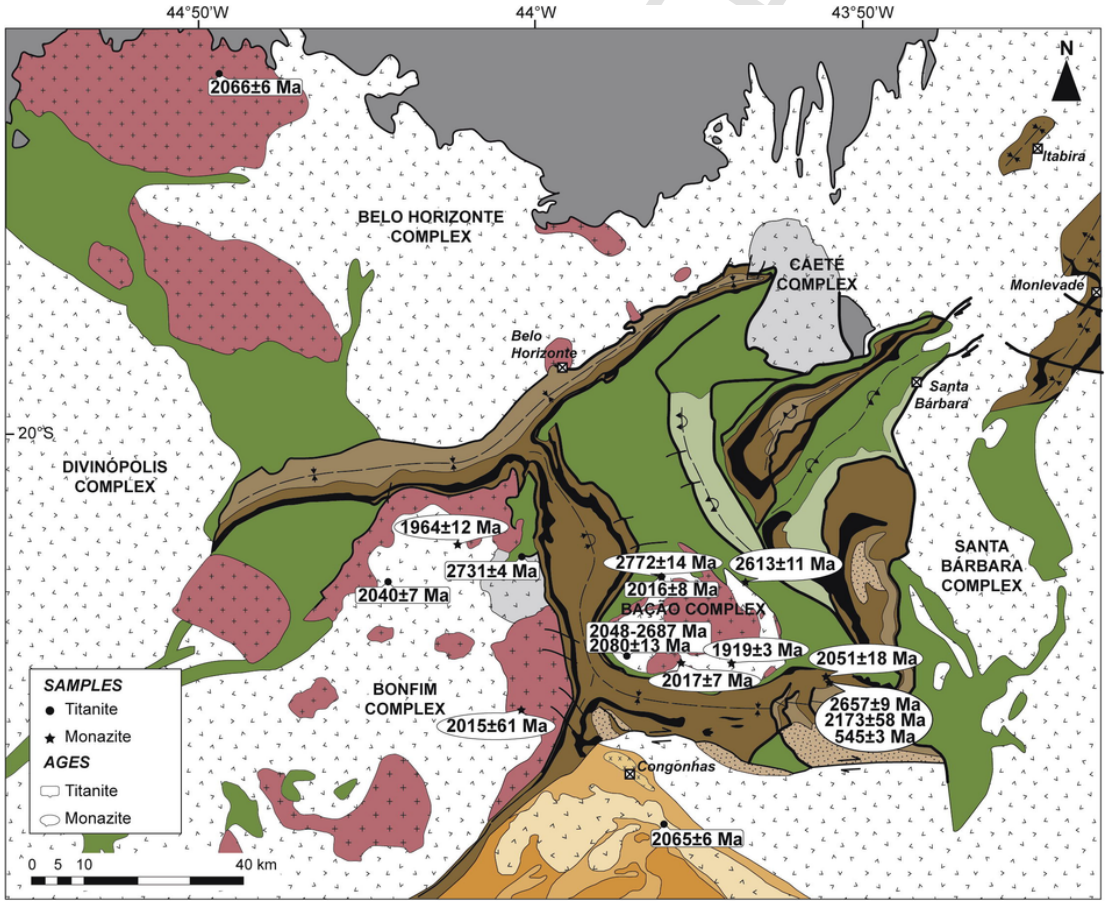

Fig. 7. Geological map of the southernmost São Francisco Craton showing all titanite and monazite ages obtained in this study (ages are compiled in Table 1). See legend in Fig. 2.

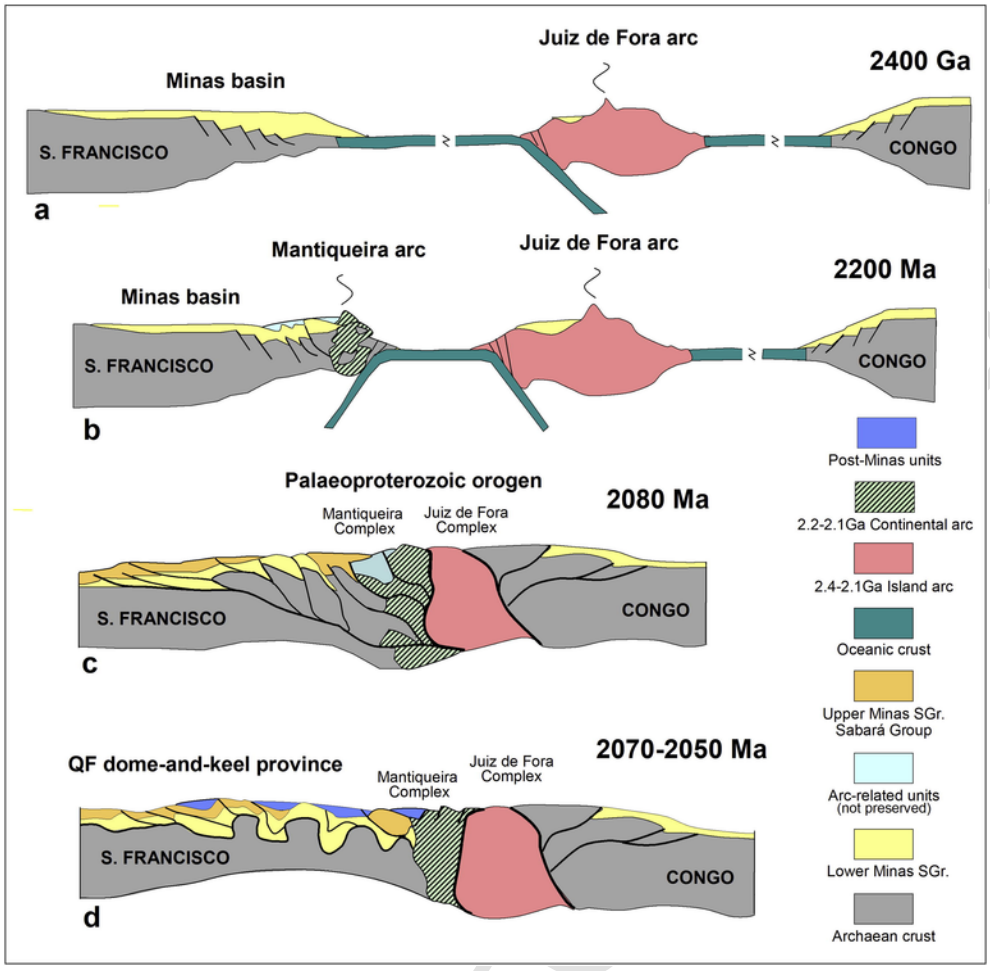

Fig. 8. Cross-sectional model (EW-oriented) illustrating the tectonic evolution of the southern São Francisco craton and its eastern margin between 2400 and 2050 Ma. a) Pre-collisonal stage, in which the Minas and Congo passive margins were separated by an ocean hosting the Juiz de Fora island arc; b) Development of the Mantiqueira continental arc and initial inversion of the Minas passive margin, in this stage converted into a back-arc setting; c) Collision of the São Francisco and Congo Archaean nuclei, involving the Juiz de Fora juvenile terrane; and d) Extensional collapse affecting the southern São Francisco foreland/back-arc zone and development of the dome-and-keel architecture that characterizes the region.

morphic studies and phase diagram modeling (Cutts et al., subm.) indicate exhumation of hot (700 °C), midcrustal (20 km deep) gneiss domes, clearly related to extension at *ca*. 2070–2050 Ma interval. Thus, combining the published structural geology/metamorphic petrology data with the widespread distribution of U–Pb titanite/monazite, we suggest that entire SSFC was affected by the crustal extension and thermal heating emanating from it. Remarkably, the titanite and monazite ages we obtained also indicates a relatively slow cooling of the SSFC, lasting from 2080 up to 1940 Ma.

Younger metamorphic ages were also determined by K–Ar biotite dating in the Passa Tempo – Campo Belo – Divinópolis complexes of the SSFC, also suggesting a protracted cooling history of craton between *ca*. 2041 and 1780 Ma (Table 1; e.g., Teixeira, 1985; Campos et al., 2003). Therefore, these data inferred slow cooling of these rocks during relaxation of isotherms following the closure of the Minas Basin and dome exhumation. The cooling rate can be estimated very approximately at about 1 °C/Ma, based on an age of 2080 ± 13 Ma for the peak of metamorphism at ~650 °C and 1745 ± 52 Ma for the closure of Pb diffusion from biotite at ~350 °C. This regional metamorphic cooling rate is supported by Tassinari et al. (2015), who evaluated the cooling rate based on multi-system isotope data, fluid inclusion microthermometry and other relevant information. Moreover, the closure temperature of titanite for slowly-cooling metamorphic event is considered to be between 600 °C (Mezger et al., 1991) and 700 °C (Scott and St-Onge, 1995; Bingen and van Breemen, 1998), reinforcing that the Palaeoproterozoic metamorphism associated with closure of the Minas Basin and dome exhumation reached amphibolite-facies condition (e.g., Jordt-Evangelista et al., 1992; Cutts et al., subm.).

5.3. *Stabilization of the São Francisco craton*

Previous studies made a case that *ca*. 100% of the SFC and its margins were built during tectonic amalgamation of Archaean blocks along with magmatic additions between 2100 and 1900 Ma; i.e., during the Palaeoproterozoic Transamazonian event (Fig. 9; e.g., Cordani et al., 1988; Teixeira et al., 2000). The magmatic processes and high-grade metamorphism played a major role in converting the São Francisco lithosphere in a stable cratonic region. For the northeastern portion of the craton, the geochronological and geological data point to accretion of continental arcs and final collision of various crustal segments (Teixeira and Fegueiredo, 1991; Sabaté et al.,

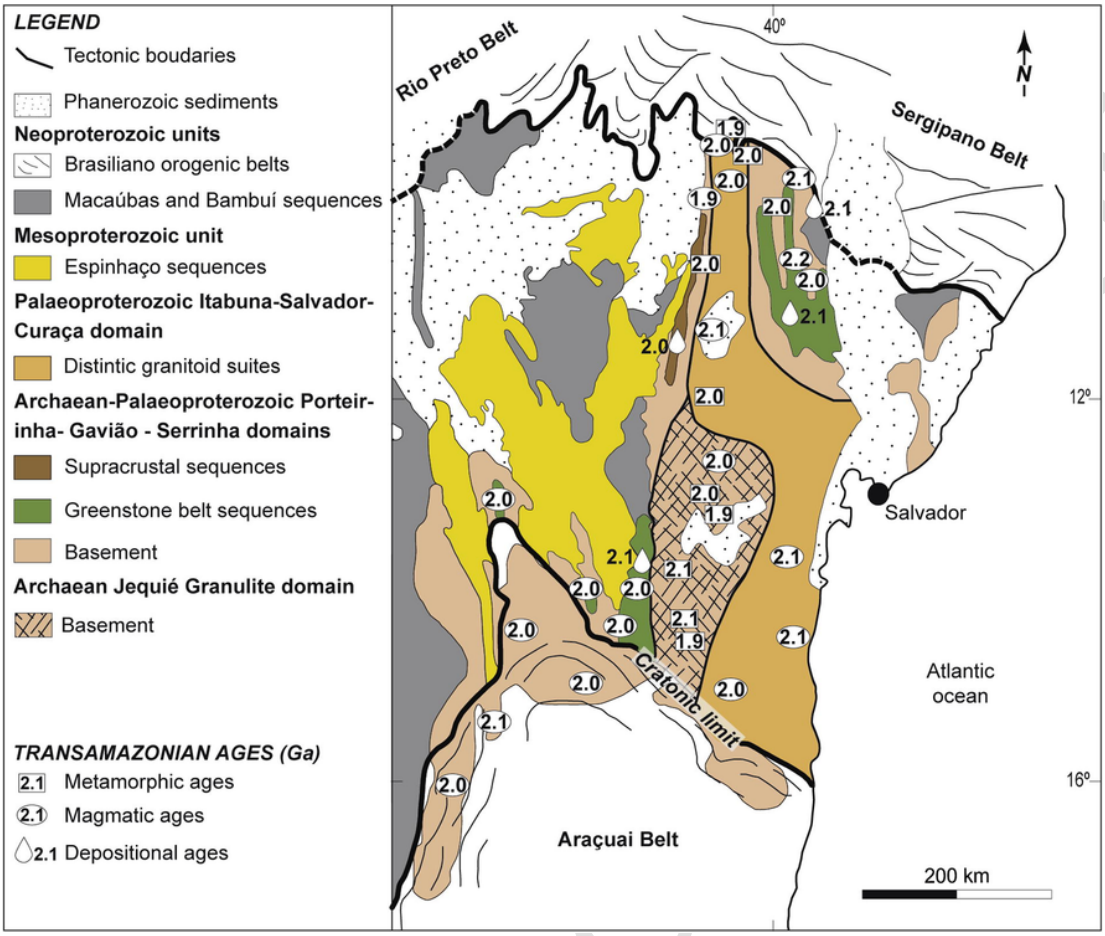

Fig. 9. Geological sketch map of the northern sector of São Francisco Craton with all available Palaeoproterozoic metamorphic and magmatic ages (ages are compiled in Table 2). Modified from Alkmim and Martins-Neto (2012). The compiled Palaeoproterozoic magmatic ages were obtained from syn- to post-collisional granitiods.

1994; Ledru et al., 1997; Silva et al., 1997; Oliveira et al., 2000; Silva et al., 2001, 2002; Delgado et al., 2003; Barbosa and Sabaté, 2004; Oliveira et al., 2004a,b, 2010, 2011). Besides this, the collisional process, which reached its climax at 2083 Ma (Peucat et al., 2011), involved first a frontal collisions among the various blocks, followed by a strong sinistral transpressional deformation of the whole system (Alves da Silva, 1994; Chauvet et al., 1997; Barbosa and Sabaté, 2004; Barbosa et al., 2012; Cruz et al., 2016).

The Palaeoproterozoic arc-related magmatism and the regional metamorphism documented in Mantiqueira Complex is also recorded along the border of the Gavião block (Fig. 9) in the northern portion of the craton (Barbosa and Sabaté, 2004; Cruz et al., 2016), meaning that sometime between *ca*. 2300 and 2100 Ma, the eastern edge of the Archaean nucleus of the SFC was converted in an active continental margin (Fig. 10), persisting as such until *ca*. 2100 Ma. Thus, the shear zone, that marks the contact of the Gavião block with the Itabuna-Salvador-Curaçá belt and Jequié block in the northern SFC as well as the contact between the Mantiqueira and Juiz de Fora Complexes (Fig. 10) in the Araçuaí orogen (SSFC margin), represents the suture zone, along which micro-continents and juvenile arcs were amalgamated during the convergence and collision of the São Francisco and Congo Archaean nuclei. This process was followed by a period of slow cooling and final stabilization of a large continental mass *ca*. 1900 Ma. A substantial portion of this continent is now preserved in the interior of the both the São Francisco and Congo cratons.

6. Conclusions

New U–Pb LA-SF-ICPMS data obtained in the SSFC reveal that the titanite and monazite growth took place during the different Neorchaean magmatic and metamorphic events between *ca*. 2760 and 2680 Ma and that they were partially or completely recrystallized and/or underwent isotopic resetting during thermal events at *ca*. 2080 and 1940 Ma. The preservation of Neoarchaean titanite and monazite indicates that the Palaeoproterozoic metamorphism associated with the closure of the Minas Basin and dome exhumation in the SSFC reached amphibolite-facies conditions with a maximum temperature between 650 and 700 °C and thus, no Palaeoproterozoic zircons were grown during this event. Using all available Palaeoproterozoic data, we can infer that a long-lived metamorphic event affected the Archaean basement in the SSFC as well as the surrounding terrains to the east and to the south, following the long-lasting westward subduction with sanukitoid-like magmatism associated in the surrounding terrains of the SSFC. This long-lived metamorphism include an episode of *syn*-collisional metamorphism between 2100 and 2070 Ma, which represents the amalgamation of the Archaean nuclei of both the São Francisco and Congo cratons, along with magmatic arcs and microcontinents. This collision led to closure of the large

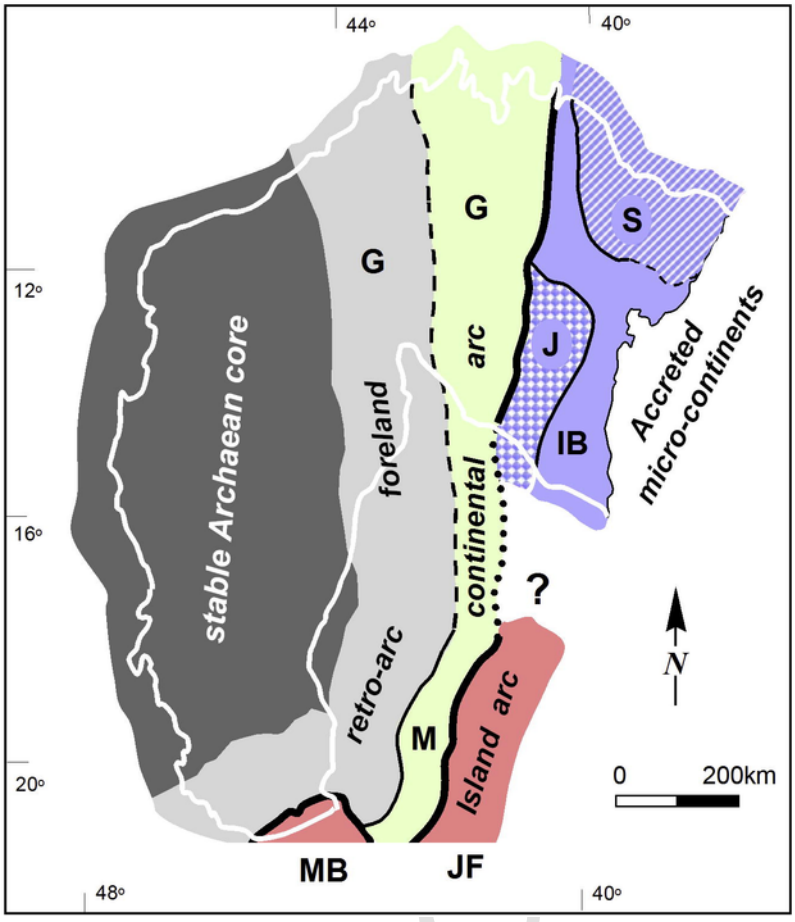

Fig. 10. Tentative reconstruction of the tectonic scenario of the São Francisco Craton and its margins after the Palaeoproterzoic collision. The Archaean stable core of the craton was bordered by a foreland/retro-arc domain and an active continental margin, represented by the Mantiqueira Complex (M) at the southern SFC margin. The accretionary zone of the Palaeoproterozoic orogen is composed of the various microcontinents of the northeastern SFC (G: Gavião block; IB: Itabuna-Salvador-Curaça belt; J: Jequié block; S: Serrinha block), as well as the Juiz de Fora (JF) and Mineiro belt (MB) juvenile terranes. Modified from Alkmim and Marshak (1998).

Palaeoproterozoic Minas basin, followed by orogenic collapse and development of a dome-and-keel architecture in the time interval between 2070 and 2050 Ma. A period of slow cooling (~1 °C/Ma) followed the stabilization of the craton and lasted until *ca*. 1940 Ma.

The timing of this long-lived thermal event overlaps well with the Palaeoproterozoic ages obtained in the four blocks of the northern part of the craton. Therefore, this Palaeoproterozoic thermal event represents the last craton-wide overprinting episode responsible for the assembly and stabilization of the craton. Taking into account the previous evolutionary models proposed for both sectors, the continuity of the massive magmatic arc around the margins of the SSFC can be represented along the Archaean blocks in the northern part of the craton. Therefore, the SSFC can be interpreted as foreland or back-arc basins formed behind to the magmatic arc, owing to the absence of the Palaeoproterozoic magmatic activities in this sector and the deposition of the syn-orogenic sedimentary sequences.

Acknowledgements

The authors wish to acknowledge funding from CNPq (401334/2012-0, 302058/2015-0, 402852/2012-5) and FAPEMIG (APQ03943, RPQ-0067-10, RPQ-0063-10) grants and Edital UFOP Auxilio a Pesquisador 2015. The authors would like to thank Camila Schuch and Livia P. V. Teixeira for their help with the titanite- and monazite-mount preparation and with instrument tuning during the course of this work. To the Microanalysis Laboratory of the Universidade Federal de Ouro Preto, a member of the Microscopy and Microanalysis Network of Minas Gerais State/Brazil/FAPEMIG, for the mineral chemistry analyses. We are also indebted to Francesco Narduzzi for his moral support and comments.

Appendix A. Supplementary data

Supplementary data associated with this article can be found, in the online version, at http://dx.doi.org/10.1016/j.precamres.2016.12.001.

References

Alkmim, F.F., 2004. O que faz de um cráton um cráton? O Cráton do São Francisco e as revelações Almeidianas ao delimitá-lo. In: Mantesso-Neto (Ed.), Geologia do Continente Sul- Americano. Evolução da obra de Fernando Flávio Marques de Almeida, Becca, São Paulo, Brazil, pp. 17–35.

Alkmim, F.F., Marshak, S., 1998. Transamazonian Orogeny in the Southern São Francisco Craton Region, Minas Gerais, Brazil: Evi-

dence for Paleoproterozoic collision and collapse in the Quadrilátero Ferrífero. Precambr. Res. 90, 29–58.
Alkmim, F.F., Martins-Neto, M.A., 2012. Proterozoic first-order sedimentary sequences of the São Francisco craton, eastern Brazil. Marine and Petroleum Geolgoy 33, 127–139.
Almeida, F.F.M., 1977. O Cráton São Francisco. Brazilian Journal of Geology 7, 349–364.
Almeida, F.F.M., Hasui, Y., Brito Neves, B.B., Fuck, R.A., 1981. Brazilian structural provinces: An introduction. Earth-Sciences Reviews 17, 1–29.
Alves da Silva, F.C., 1994. Etude structurale de la greenstone-belt Paléoproterozoique du Rio Itapicuru (Bahia, Brésil). Unpublished Ph.D. Thesis Université d'Orléans, Orléans, France. 307 pp.
Ávila, C.A., 2000. Geologia, petrografia e geocronologia de corpos plutônicos Paleoproterozóicos da borda meridional do Cráton São Francisco, região de São João del Rei, Minas Gerais. Unpublished Ph.D. Thesis Universidade Federal do Rio de Janeiro, Rio de Janeiro, Brazil. 401 pp.
Ávila, C.A., Teixeira, W., Pereira, R.M., 2004. Geologia e petrografia do Quartzo Monzodiorito Glória, Cinturão Mineiro, porção sul do Craton São Francisco, Minas Gerais. Arquivos do Museu Nacional 62, 83–98.
Ávila, C.A., Cherman, A.F., Valença, J.G., 2008. Dioritos Brumado e Rio Grande: geologia e relação com o metamorfismo paleoproterozóico do Cinturão Mineiro, borda meridional do Cráton São Francisco, Minas Gerais. Arquivos do Museu Nacional 67, 248–277.
Ávila, C.A., Teixeira, W., Cordani, U.G., Veloso Moura, C.A., Pereira, R.M., 2010. Rhyacian (2.23 – 2.20 Ga) juvenile accretion in the southern São Francisco Craton, Brazil: Geochemical and isotopic evidence form the Serrinha magmatic suite, Mineiro belt. J. S. Am. Earth Sci. 29, 464–482.
Ávila, C.A., Teixeira, W., Bongiolo, E.M., Dussin, I.A., Almeida Teixeira.Vieira, T., 2014. Rhyacian evolution of subvolcanic and metasedimentary rocks of the southern segment of the Mineiro belt, São Francisco Craton, Brazil. Precambr. Res. 243, 221–251.
Babinski, M., Chemale Jr., F., Van Schumus, W.R., 1995. The Pb/Pb age of the Minas Supergroup carbonate rocks, Quadrilátero Ferrífero, Brazil. Precambr. Res. 72, 235–245.
Baltazar, O.F., Zuccheti, M., 2007. Lithofacies associations and structural evolution of the Archean Rio das Velhas greenstone belt, Quadrilátero Ferrífero, Brazil: A review of the setting of gold deposits. Ore Geol. Rev. 32, 1–2.
Barbosa, J.S.F., Nicollet, C., Kienast, J.R., Fornari, A., 2000. Archean Al-Mg granulites with hercinite and quartz, Jequié Complex, Bahia, Brazil. In: 31 International Geological Congress, Rio de Janeiro, Brazil, CD-ROM.
Barbosa, J.S.F., Martin, H., Peucat, J-J., 2000. Archean vs. Paleoproterozoic crustal evolution of the Laje, Mutuipe, Brejões and Santa Inês Region, Jequié Complex, Bahia, Brazil. In: 31 International Geological Congress, Rio de Janeiro, Brazil, CD-ROM.
Barbosa, J.S.F., Kienast, J.R., 2000. Sapphirine-bearing Al-Mg Gneisses, Itabuna Belt, Bahia, Brazil. In: 31 International Geological Congress, Rio de Janeiro, Brazil, CD-ROM.
Barbosa, J.S.F., Sabaté, P., 2002. Geological features and the Paleoproterozoic collision of the four Archean crustal segments of the São Francisco Craton, Bahia, Brazil. A synthesis. Anais da Academia Brasileira de Ciências 74, 343–359.
Barbosa, J.S.F., Sabaté, P., 2004. Archean and Paleoproterozoic crust of the São Francisco Craton, Bahia, Brazil: Geodynamic features. Precambr. Res. 133, 1–27.
Barbosa, J.S.F., Martin, H., Peucat, J.-J., 2004. Palaeoproterozoic dome-forming structures related to granulite-facies metamorphism, Jequié block, Bahia, Brazil: Petrogenetic approaches. Precambr. Res. 135, 105–131.
Barbosa, J.S.F., Peucat, J.-J., Martin, H., Silva, F.C.A., Corrêia-Gomes, L.C., Sabaté, P., Marinho, M.M., Fanning, C.M., Moraes, A.M.V., 2008. Petrogenesis of the late-orogenic Bravo granite and surrounding high-grade country rocks in the Paleoproterozoic orogen of Itabuna-Salvador-Curaçá Block, Bahia. Brazil. Precambrian Research 167 (3), 35–52.
Barbosa, J.S.F., Mascarenhas, J.F., Correa-Gomes, L.C., Dominguez, L.M., Santos de Souza, J., 2012. Geologia da Bahia: Pesquisa e Atualização. Série publicações especiais, Salavador, CBPM. p. 559.
Barbosa, N.S., Teixeira, W., Ávila, C.A., Montecinos, P.M., Bongiolo, E.M., 2015. 2.17–2.10 Ga plutonic episodes in the Mineiro belt, São Francisco Craton, Brazil: U-Pb ages, geochemical constraints and tectonics. Precambr. Res. 270, 204–225.
Bastos Leal, L.R.B., Teixeira, W., Macambira, M.J.B., Cordani, U., Cunha, J.C., 1996. Evolução crustal dos terrenos TTGs arqueanos do Bloco do Gavião, Craton do São Francisco: Geocronologia U-Pb Shrimp e Pb-Pb em zircões. In: 32 Congresso Brasileiro de Geologia, Salvador, Brazil. Sociedade Brasileira de Geologia, pp. 539–541. Abstract 6.
Bastos Leal, L.R., 1998. Geocronologia U/Pb (SHRIMP), 207Pb-206Pb, Rb-Sr, Sm-Nd e K-Ar dos terrenos granito-greenstone do Bloco Gavião: Implicações para a evolução Arqueana e Paleoproterozóica do Cráton do São Francisco, Brasil. Unpublished Ph.D Thesis. In: Instituto de Geociências, Universidade de São Paulo, São Paulo, Brazil. 176 pp.
Belo de Oliveira, O.A., Teixeira, W., 1990. Evidências de uma tectónica tangencial proterozóica no Quadrilátero Ferrífero. In: 36 Congresso Brasileiro de Geologia, Natal, Brazil. Sociedade Brasileira de Geologia, Abstract 6. pp. 2589–2604.
Bingen, B., van Breemen, O., 1998. U-Pb monazite ages in amphibolite- to granulite-facies orthogneiss reflect hydrous mineral breakdown reactions: Sveconorwegian Province of SW Norway. Contrib. Miner. Petrol. 132, 336–353.
Brueckner, H.K., Cunningham, D., Alkmin, F.F., Marshak, S., 2000. Tectonic implications of Precambrian Sm–Nd dates from the southern São Francisco craton and adjacent Araçuaí and Ribeira belts, Brazil. Precambr. Res. 99, 255–269.
Campos, J.C.S., Carneiro, M.A., Baset, M.A.S., 2003. U-Pb evidence for late Neoarchean crustal reworking in the southern São Francisco Craton (Minas Gerais, Brazil). Anais da Academia Brasileira de Ciências 75 (4), 497–511.
Carneiro, M.A., 1992. O complexo Metamórfico do Bonfim Setentrional. 45. REM: Revista da Escola de Minas, Universidade Federal de Ouro Preto, Ouro Preto. pp. 155–156.
Carvalho, M.J., Oliveira, E.P., 2003. Geologia do Tonalito Itareru, Bloco Serrinha, Bahia: Uma intrusão sin-tectônica do início da colisão continental no segmento norte do Orógeno Itabuna–Salvador–Curaçá. Revista Brasileira de Geociências 33, 55–68.
Chauvet, A., Guerrot, C., Alves da Silva, F., Faure, M., 1997. Géochronologie 207Pb/206Pb et 40Ar/39Ar des granites paléoprotérozoiques de la ceinture de roches vertes du Rio Itapicuru (Bahia, Brésil). Comptes Rendus de l'Académie des Sciences Paris, 324, série Iia, 293–300.
Chemale Jr., F., Rosière, C.A., Endo, I., 1994. The tectonic evolution of the Quadrilátero Ferrífero, Minas Gerais, Brazil. Precambr. Res. 65, 25–54.

Cheilletz, A., Féraud, G., Giuliani, G., Ruffet, G., 1993. Emerald dating through $^{40}Ar/^{39}Ar$ step-heating and laser spot analysis of syngenetic phlogopite. Earth Planet. Sci. Lett. 120, 473–485.

Cherman, A.F., 1999. Geologia e petrografia de áreas dos Greenstone Belt Rio Capivari-Rio das Mortes e Itumirim-Tiradentes e rochas granitóides associadas, entre Nazareno e Lavras (Estado de Minas Gerais). Unpublished Msc. Dissertation Universidade Federal do Rio de Janeiro, Rio de Janeiro, Brazil. 161 pp.

Cherniak, D.J., 1993. Lead diffusion in titanite and preliminary results on the effects of radiation damage on Pb transport. Chem. Geol. 110, 177–194.

Cherniak, D.J., Watson, E.B., 2001. Pb diffusion in zircon. Chem. Geol. 172, 5–24.

Childe, F., Doig, R., Gariepy, C., 1993. Monazite as a metamorphic chronometer, south of the Grenville Front, western Quebec. Canadian Journal Earth Science 30, 1056–1065.

Conceição, H., 1990. Pétrologie du massif syénitique d'Itiuba, contribution à l'etude minéralogique des roches alcalines dans l'Etat de Bahia (Brésil). Unpublished Ph.D. Thesis Paris Sud University, Orsay, France. 393 pp.

Conceição, R.V., Rosa, M.L.S., Nardi, L.V., Conceição, H., Lafon, J.M., Soliani, E., Oberli, F., Maier, M., Martin, H., 1999. Geochronology and isotopic signature of the Paleoproterozoic Santanápolis syenite (Bahia, Brazil). In: Second South American Symposum on Isotope Geology. Cordoba, Argentina, Actas, pp. 171–178.

Conceição, H., Rios, D.C., Rosa, M.L.S., Davis, D.W., Dickin, A., MCreath, I., Marinho, M.M., Macambira, M.J.B., 2002. Zircon geochronology and petrology of alkaline – potassic syenites, southwestern Serrinha block, East São Francisco Craton, Brazil. International Geology Review 44, 117–136.

Cordani, U.G., Teixeira, W., Tassinari, C.C.G., Kawashita, K., Sato, K., 1988. The growth of the Brazilian shield. Episodes 11, 163–167.

Correa Gomes, L.C., 2000. Evolução dinâmica da zona de cisalhamento neoproterozóica de Itabuna-Itaju do Colonia e do magmatismo fissural alcalino associado (SSE do Estado da Bahia, Brasil). Unpublished Ph.D. Thesis Universidade Estadual de Campinas, Campinas, Brazil. 362 pp.

Costa, F.G., 2008. Petrogênese do granodiorito Fazenda Gavião: registro de uma colisão arco-continente no greenstone belt do Rio Itapicuru, Craton do São Francisco, Bahia. Unpublished Mcs. dissertation Instituto de Geociências, Universidade Estadual de Campinas, Campinas, Brazil.

Cruz Filho, B.E., Conceição, H., Rosa, M.L.S., Rios, D.C., Macambira, M.J.B., Marinho, M.M., 2005. Geocronologia e assinatura isotópica (Rb–Sr e Sm–Nd) do batólito trondhjemítico Nordestina, núcleo Serrinha, nordeste do estado da Bahia. Revista Brasileira de Geociências 35, 1–8.

Cruz, S.C.P., Barbosa, J.S.F., Pinto, M.S., Peucat, J.-J., Paquette, J.L., Santos de Souza, J., de Souza Martins, V., Chemale Jr., F., Carneiro, M.A., 2016. The Siderian-Orosirian magmatism in the Archean Gavião Paleoplate, Brazil: U–Pb geochronology, geochemistry and tectonic implications. J. S. Am. Earth Sci. http://dx.doi.org/10.1016/j.jsames.2016.02.007.

Cutts, K., Lana, C., Alkmim, F.F., Moreira, H., Coelho, V., submitted. Metamorphism and exhumation of basement gneiss domes in the Quadrilátero Ferrífero, SE Brazil: Implication for dome-and-keel formation. *Precambrian Research*.

Delgado, I.M., Souza, J.D., Silva, L.C., Silveira Filho, N.C., Santos, R.A., Pedreira da Silva, A., Guimarães, J.T., Angelim, L.A.A., Vasconcelos, A.M., Gomes, I.P., Lacerda Filho, J.W., Valente, C.R., Perrotta, M.M., Heineck, C.A., 2003. Geotectônica do Escudo Atlântico. In: Bizzi, L.A., Schobbenhaus, C., Vidotti, R.M., Gonçalves, J.H. (Eds.), Geologia, Tectônica e Recursos Minerais do Brasil. CPRM, Brasilia, Brazil, pp. 227–334.

D'el-Rey Silva, L.J.H., Oliveira, J.G., Gaal, E.G., 1996. Implication of the Caraíba deposit's structural controls on the emplacement of the Cu-bearing hypersthenites of the Curaçá Valley. Bahia-Brazil. Revista Brasileira de Geociencias 26 (3), 181–196.

D'el-Rey Silva, L.J.H., Dantas, E.L., Guimarães Teixeira, J.B., Laux, J.H., da Silva, M.G., 2007. U-Pb and Sm–Nd geochronology of amphibolites from the Curaçá Belt, São Francisco Craton, Brazil: Tectonic implications. Gondwana Res. 12, 454–467.

Dorr, J.V.N., 1969. Physiographic, stratigraphic and structural development of the Quadrilátero Ferrírfero, Minas Gerais, Brazil. USGS Prof. Paper 641-A, pp. 110.

Duarte, B.P., Valente, S.C., Campos Neto, M.C., 2004. Petrogenesis of the orthogneisses of the Mantiqueira Complex, Central Ribeira Belt, SE Brazil: an archean to basement unit reworked during the Pan-African orogeny. Gondwana Res. 7, 437–450.

Duarte, B.P., Heilbron, M., Ragatky, D., Valente, S.C., 2005. Mantiqueira and Juiz de Fora Complexes: Reworked Basement Units Within A Western Gondwana Mobile Belt in Brazil. In: Gondwana 12. Academia Nacional de Ciências, Mendoza, Argentina, p. 142.

Farina, F., Albert, C., Lana, C., 2015. The Neoarchean transition between medium- and high-K granitoids: clues from the Southern São Francisco Craton (Brazil). Precambr. Res. 266, 375–394.

Farina, F., Albert, C., Martínez Dopico, C., Aguilar, C., Moreira, H., Hippertt, J.P., Cutts, K., Alkmim, F.F., Lana, C., 2015. The Archean-Paleoproterozoic evolution of the Quadrilátero Ferrífero (Brasil): current models and open questions. J. S. Am. Earth Sci.http://dx.doi.org/10.1016/j.jsames.2015.10.015.

Feybesse, J.L., Johan, V., Triboulet, C., Guerrot, C., Mayaga-Mikolo, F., Bouchot, V., Eko N'dong, J., 1998. The West Central African belt: a model of 2.5–2.0 Ga accretion and two-phase orogenic evolution. Precambr. Res. 87, 161–216.

Pimentel, D.P., Fuck, M., Costa, R.A., Rosiere, A.G., 1998. Geology and Sm-Nd isotopic data for the Mantiqueira and Juiz de Fora complexes (Ribeira belt) in the Abre Campo-Manhuaçu region, Minas Gerais, Brazil. In: Proceedings of the 14th International Conference on Basement Tectonics, Ouro Preto, Brazil. pp. 21–23.

Gascoyne, M., 1986. Evidence for the stability of the potential nuclear waste host, sphene, over geological time, from uranium-lead ages and uranium-series measurements. Appl. Geochem. 1, 199–210.

Hartmann, L.A., Endo, I., Suita, M.T.F., Santos, J.O.S., Frantz, J.C., Carneiro, M.A., Naughton, N.J., Barley, M.E., 2006. Provenance and age delimitation of Quadrilátero Ferrífero sandstones based on zircon U-Pb isotopes. J. S. Am. Earth Sci. 20, 273–285.

Hawkins, D.P., Bowring, S.A., 1997. U-Pb systematics of monazite and xenotime: case studies from the Paleoproterozoic of the Grand Canyon, Arizona. Contrib. Miner. Petrol. 127, 87–103.

Heilbron, M., Mohriak, W., Valeriano, C.M., Milani, E., Almeida, J.C.H., Tupinambá, M., 2000. From collision to extension: the roots of the Southeastern continental margin of Brazil. In: In: Talwani, Mohriak (Eds.), Atlantic Rifts and Continental Margin. AGU Geophysical Monograph, Series. vol. 115, pp. 1–32.

Heilbron, M., Machado, N., Duarte, B.P., 2001. Evolution of the Paleoproterozoic Transamazonian Orogen in SE Brazil: A view from the Neoproterozoic Ribeira Belt. In: Abstracts, GAC-MAC Joint Annual Meeting, St. Johns, Canada. vol. 26. 61.

Heilbron, M., Duarte, B.P., Valeriano, C.M., Simonetti, A., Machado, N., Nogueira, J.R., 2010. Evolution of reworked Paleoproterozoic basement rocks within the Ribeira belt (Neoproterozoic), SE-Brazil, based on U-Pb geochronology: Implications for paleogeographic reconstrutions of the São Francisco-Congo paleocontinet. Precambr. Res. 178, 136–148.

Hermann, J., Rubatto, D., 2003. Relating zircon and monazite domains to garnet growth zones: age and duration of granulite facies metamorphism in the Val Malenco lower crust. J. Metamorph. Geol. 21, 833–852.

Hippertt, J.F., Borba, R.P., Nalini Jr., H.A., 1992. O contacto Formação Moeda-Complexo do Bonfim: Uma zona de cislhamento normal na borda oeste do Quadrilátero Ferrífero, MG. Vol. 45. REM: Revista da Escola de Minas, Universidade Federal de Ouro Preto (Brazil). pp. 32–34.

Hippertt, J.F., 1994. Structure indicative of helicoidal flow in a migmatitic diapir (Bação Complex, southeastern Brazil). Tectonophysics 234, 169–996.

Jordt-Evangelista, H., Alkmim, F.F., Marshak, S, 1992. Metamorfismo progressivo e a ocorrência dos três polimorfos de Al2SiO5 (Cianita, Andaluzita e Silimanita) na formação Sabará em Ibirité, Quadrilátero Ferrífero, MG. vol. 45. REM: Revista da Escola de Minas, Ouro Preto, 151–160 (1 e 2).

Ladeira, E.A., 1980. Metallogenesis of gold at the Morro Velho mine and in the Nova Lima district, Quadrilátero Ferrífero, Minas Gerais. Unpublished Ph.D. Thesis University of Western Ontario, Canada. 272.

Lana, C., Alkmim, F.F., Armstrong, R., Scholz, R., Romano, R., Nalini Jr., H.A., 2013. The ancestry and magmatic evolution of Archean TTG rocks of the Quadrilátero Ferrífero province, southeast Brazil. Precambr. Res. 231, 157–173.

Leahly, G.A.S., Conceição, H., Rosa, M.L.S., Macambira, M.J.B., Martin, H., Paim, M.M., Santos, E.B., Bastos Leal, L.R., 1998. Maciço Sienítico de Ceraima (Sudoeste da Bahia): Idade, petrografia e geoquimica do magmatismo pós-orogênico alcalino potássico com afinidade lamprofírica. In: Conceição, H. (Ed.), Contribuição ao Estudo dos Granitos e Rochas Correlatas. Nucleo Bahia-Sergipe, Special Publication, Sociedade Brasileira de Geologia, pp. 1–77.

Ledru, P., Cocherie, A., Barbosa, J.S.F., Johan, V., Onsted, T., 1994. Age du métamorphisme granulitique dans le Craton du São Francisco (Brésil). Implications sur la nature de l'orogène transmazonien. Comptes Rendus de l'Académie des Sciences Paris 211, 120–125.

Ledru, P., Johan, V., Milesi, J.P., Tegyey, M., 1994. Evidence for a 2 Ga continental accretion in the circum-south Atlantic provinces. Precambr. Res. 69, 169–191.

Ledru, P., Milési, J.P., Johan, V., Sabaté, P., Maluski, H., 1997. Foreland basins and gold-bearing conglomerates: a new model for the Jacobina Basin (São Francisco Province, Brazil). Precambr. Res. 86, 155–176.

Lee, J.K.W., Williams, I.S., Ellis, D.J., 1997. Pb, U and Th diffusion in natural zircon. Nature 390, 159–161.

Leite, C.M.M., Barbosa, J.S.F., Gonçalves, P., Nicollet, C., Sabaté, P., 2009. Petrological evolution of silica-undersaturated sapphirine-bearing granulite in the Paleoproterozoic Salvador-Curaçá Belt, Bahia, Brazil. Gondwana Res. 15, 49–70.

Machado, N., Carneiro, M., 1992. U-Pb evidence of late Archean tectono-thermal activity on the southern São Francisco shield, Brazil. Can. J. Earth Sci. 29 (11), 2341–2346.

Machado, N., Noce, C.M., Ladeira, E.A., Belo de Oliveira, O., 1992. U-Pb Geochronology of Archean magmatism and Proterozoic metamorphism in the Quadrilátero Ferrífero, southern São Francisco craton, Brazil. Geol. Soc. Am. Bull. 104, 1221–1227.

Machado, N., Schrank, A., Noce, C.M., Gauthier, G., 1996. Ages of detrital zircon from Archean-Paleoproterozoic sequences Implications for Greenstone Belt setting and evolution of a Transamazonian foreland basin in Quadrílatero Ferrífero, southeastern Brazil. Earth Planet. Sci. Lett. 141, 259–276.

Marinho, M.M., 1991. La Séquence Volcano-Sedimentaire de Contendas-Mirante et la Bordure Occidentale du Bloc Jequié (Cráton du São Francisco-Brésil): Un exemple de Transition Archéean-Protérozoique. Unpublished Ph.D. Thesis Blaise Pascal University, Clermont Ferrand, France. 388.

Marshak, S., Alkmim, F.F., Jordt-Evangelista, H., 1992. Proterozoic crustal extension and the generation of the dome-and-keel structure in an Archean granite – greestone terrane. Nature 357, 491–493.

Marshak, S., Tinkham, D., Alkmim, F.F., Brueckner, H.K., Bornhorst, T., 1997. Dome-and-keel provinces formed during Paleoproterozoic orogenic collapse-Diapir clusters or core complexes? Examples from the Quadrilátero Ferrífero (Brazil) and the Penokean Orogen (USA). Geology 25, 415–418.

Mello, E.F., Xavier, R.P., McNaughton, N.J., Hagemann, S.G., Fletcher, I., Snee, L., 2006. Age constraints on felsic intrusions, metamorphism and gold mineralization in the Paleoproterozoic Rio Itapicuru greenstone belt, NE Bahia State, Brazil. Miner. Deposita 40, 849–866.

Mezger, K., Rawnsley, C.M., Bohlen, S.R., Hanson, G.N., 1991. U-Pb garnet, titanite, monazite, and rutile ages: Implications for the duration of high-grade metamorphism and cooling histories, Adirondack Mountains, New York. J. Geol. 99, 415–428.

Mezger, K., Essene, E.J., van der Pluijm, B.A., Halliday, A.N., 1993. U-Pb geochronology of the Grenville Orogen of Ontario and New York: constraints on ancient crustal tectonics. Contrib. Miner. Petrol. 114, 13–26.

Moreira, H., Lana, C., Nalini Jr., H.A., 2016. The detrital zircon record of an Archaean convergent basin in the Southern São Francisco Craton, Brazil. Precambr. Res. 272, 84–99.

Mougeot, R., 1996. Etude de la limite Archéen-Protérozoique et des mineralisations Au, ±U associées. Exemples de la région de Jacobina (Etat de Bahia, Brésil) et de Carajas (Etat de Para, Brésil). Unpublished Ph.D. Thesis Montpellier II University, Montpellier, France. 301.

Noce, C.M., 1995. Geocronologia dos eventos magmáticos, sedimentares e metamórficos na região do Quadrilátero Ferrífero, Minas Gerais. Unpublished Ph.D. Thesis University of São Paulo, São Paulo, Brazil. 129.

Noce, C.M., Machado, N., Teixeira, W., 1998. U-Pb geochronology of gneisses and granitoids in the Quadrilátero Ferrífero (Southern São Francisco Craton): age constraints for Archean and Paleoproterozoic magmatism and metamorphism. Rev. Bras. Geociências 28, 95–102.

Noce, C.M., Teixeira, W., Quéméneur, J.J.G., Martins, V.T.S., Bolzachini, E., 2000. Isotopic signatures of Paleoproterzoic granitoids from the southern São Francisco Craton and implications for the evolution of the Transamazonian Orogeny. J. South Am. Sci. 13, 225–239.

Noce, C.M., Zuccheti, M., Baltazar, O.F., Armstrong, R., Dantas, E., Renger, F.E., Lobato, L.M., 2005. Age of felsic volcanism and the role of ancient continental crust in the evolution of the Neoarchean Rios da Velhas Greenstone belt (Quadrilátero Ferrífero, Brazil): U-Pb zircon dating of volcaniclastic graywackes. Precambr. Res. 141, 67–82.

Noce, C.M., Pedrosa-Soares, A.C., Silva, L.C., Armstrong, R., Piuzana, D., 2007. Evolution of polycyclic basement complexes in the Araçuaí orogeny, based on U-Pb SHRIMP data: implications for Brazil – Africa links in Paloeproterozoic time. Precambr. Res. 159, 60–78.

Nutman, A.P., Cordani, U.G., Sabaté, P., 1994. SHRIMP U-Pb ages of detrital zircons from the Early Proterozoic Contendas-Mirante supracrustal belt, São Francisco Craton, Bahia, Brazil. J. S. Am. Earth Sci. 7, 109–114.

Oliveira, E.P., Lafon, J.M., 1995. Age of ore-rich Caraíba and Medrado. In: Congresso Brasileiro de Geoquimica. CD-ROM, Bahia, Brazil.

Oliveira, E.P., Lafon, J.M., Souza, Z.S., 1998. A Paleoproterozoic age for the Rio Capim volcano-plutonic sequence, Bahia, Brazil: whole-rock Pb-Pb, Pb-evaporation and U-Pb constraints. In: 40 Congresso Brasileiro de Geologia, Sociedade Brasileira de Geologia, Belo Horizonte, Brazil. p. 14.

Oliveira, E.P., Souza, Z.S., Corrêa Gomes, L.C., 2000. U-Pb dating of deformed mafic dyke and host gneiss: implications for understanding reworking processes on the western margin of the Archaean Uau Block, NE São Francisco Craton, Brazil. Rev. Bras. Geociências 30, 149–152.

Oliveira, E.P., Mello, E.F., McNaughton, N.J., 2002. Reconnaissance U-Pb geochronology of early Pre-cambrian quartzites from the Caldeirão belt and their basement, NE São Francisco Craton, Bahia, Brazil: implications for the early evolution of the Palaeoproterozoic Salvador-Curaçã Orogen. J. S. Am. Earth Sci. 15, 284–298.

Oliveira, E.P., Mello, E.F., McNaughton, N.J., 2002. SHRIMP U-Pb geochronology of early Precambrian quartzite and its basement (Caldeirão Belt), NE São Francisco Craton, Bahia, Brazil. J. S. Am. Earth Sci. 15, 349–362.

Oliveira, E.P., Carvalho, M.J., McNaughton, N.J., 2004. Evolução do segmento norte do Orógeno Itabuna – Salvador – Curaçá: Cronologia da acresção de arcos, colisão continental e escape de terrenos. Revista Geologia USP – Série Científica 4, 41–53.

Oliveira, E.P., Windley, B.F., McNaughton, N.J., Pimentel, M., Fletcher, I.R., 2004. Contrasting copper and chromium metallogenic evolution of terranes in the Palaeoproterozoic Itabuna–Salvador–Curaçá Orogen, São Francisco Craton, Brazil: new zircon (SHRIMP) and Sm–Nd (model) ages and their significance for orogen-parallel escape tectonics. Precambr. Res. 128, 143–165.

Oliveira, E.P., McNaughton, N.J., Armstrong, R., 2010. Mesoarchaean to Palaeoproterozoic growth of the northern segment of the Itabuna-Salvador-Curaçá Orogen, São Francisco Craton, Brazil. In: In: Kusky, T.M., Zhai, M.-G., Xiao, W. (Eds.), The Evolving Continents: Understanding Processes of Continental Growth. vol. 338. Geological Society of London, Special Publications, pp. 263–286.

Oliveira, E.P., Souza, Z.S., McNaughton, N.J., Lafon, J.-M., Costa, F.G., Figueiredo, A.M., 2011. The Rio Capim volcanic–plutonic–sedimentary belt, São Francisco Craton, Brazil: geological, geochemical and isotopic evidence for oceanic arc accretion during Palaeoproterozoic continental collision. Gondwana Res. 19, 735–750.

Parrish, R.R., 1990. U-Pb dating of monazite and its application to geological problems. Can. J. Earth Sci. 27, 1431–1450.

Peucat, J.J., Barbosa, J.S.F., Araújo Pinho, I.C., Paquette, J.L., Martin, H., Fanning, C.M., Menezes Leal, A.B., Cruz, C.P.S., 2011. Geochronology of granulites from the south Itabuna-Salvador-Curaçá Block, São Francisco Craton (Brazil): Nd isotopes and U-Pb zircon ages. J. S. Am. Earth Sci. 31, 397–413.

Porada, H., 1989. Pan-African rifting and orogenesis in southern to equatorial Africa and eastern Brazil. Precambr. Res. 44, 103–136.

Ragatky, C.D., Tupinambá, M., Heilbron, M., Duarte, B.P., Valladares, C.S., 1999. New Sm/Nd isotopic data from pre-1.8 Ga Basement rocks of Central Ribeira Belt, SE Brazil. In: South-American Symposium on Isotope Geology, Córdoba, Argentina. Actas 2. 346, 348.

Renger, F.E., Noce, C.M., Romano, A.W., Machado, N., 1995. Evolução sedimentar do Supergrupo Minas: 500 Ma de registro geológico no Quadrilátero Ferrífero, Minas Gerais, Brasil. Geonomos 2 (1), 1–11.

Rios, D.C., Davis, D.W., Conceição, H., Macambira, M.J.B., Peixoto, A.A., Cruz Filho, B.E., Oliveira, L.L., 2000. Ages of granites of the Serrinha Nucleus, Bahia (Brazil): an overview. Rev. Bras. Geociências 30, 74–77.

Rios, D.C., 2002. Granitogênese no Núcleo Serrinha, Bahia, Brasil: Geocronologia e Litogeoquímica. Unpublished Ph.D. Thesis. In: Instituto de Geociências, Universidade Federal da Bahia, Salvador, Brazil.

Rios, D.C., Conceição, H., Davis, D.W., Plá Cid, J., Rosa, M.L.S., Macambira, M.J.B., McReath, I., Marinho, M.M., Davis, W.J., 2007. Paleoproterozoic potassic–ultrapotassic magmatism: Morro do Afonso syenite pluton, Bahia, Brazil. Precambr. Res. 154, 1–30.

Rios, D.C., Davis, D.W., Conceição, H., Rosa, M.L.S., Davis, W.J., Dickin, A.P., Marinho, M.M., Stern, R., 2008. 3.65–2.10 Ga history of crust formation from zircon geochronology and isotope geochemistry of the Quijingue and Euclides plutons, Serrinha nucleus, Brazil. Precam. Res. 167, 53–70.

Romano, R., Lana, C., Alkmim, F.F., Stevens, G., Armstrong, R., 2013. Stabilization of the southern portion of the São Francisco Craton, SE Brazil, though a long-lived period of potassic magmatism. Precambr. Res. 224, 143–159.

Rosa, M.I.S., Conceição, H., Paim, M.M., Santos, E.B., Alves da Silva, F.C., Leahy, G.A.S., Bastos Leal, L.R., 1996. Magmatismo potássico/ultrapotássico pós a tardi-orogênico (associado à subducção) no oeste da Bahia: Batólito monzosienítico de Guanambi-Urandi e os sienitos de Correntina. Geochim. Bras. 10, 27–42.

Rosa, M.L.S., Conceição, H., Oberli, F., Meier, M., Martin, H., Macambira, M.J.B., Santos, E.B., Paim, M.M., Leahy, G.A.S., Leal, L.R.B., 2000. Geochronology (U–Pb/Pb–Pb) and isotopic signature (Rb–Sr/Sm–Nd) of the Paleoproterozoic Guanambi batolith, southwestern Bahia State (NE Brazil). Rev. Bras. Geociências 30 (1), 62–65.

Rubatto, D., Williams, I.S., Buick, I.S., 2001. Zircon and monazite response to prograde metamorphism in the Reynolds Range, central Australia. Contrib. Miner. Petrol. 140, 458–468.

Sabaté, P., Peucat, J-J., Melo, R.C., Pereira, L.H.M., 1994. Datação por Pb-evaporação de mono-zircão em ortognaisse do Complexo Caraíba: Expressão do acrescimento crustal transamazônico do Cinturão Salvador-Curaçá (Cráton do São Francisco, Bahia, Brasil). In: 388 Congresso Brasileiro de Geologia, Sociedade Brasileira de Geologia, Camboriú. vol. 1, pp. 219–220.

Santos Pinto, M.A., 1996. Le Recyclage de la Croûte Continentale Archéene: Exemple du Bloc du Gavião-Bahia, Brésil. Unpublished Ph.D. Thesis Rennes I University, Rennes, France. 193.

Schrank, A., Souza Filho, C.R., Roig, H.L., 1990. Novas Observações sobre as Rochas Ultramáficas do Grupo Quebra Osso e Formacão Córrego dos Boiadeiros, Greenstone Belt Rio Velhas – MG. 1. Cadernos Instituto de Geociências – Universidade Estadual de Campinas. p. 6–29.

Machado, A., 1996. Idades U-Pb em monazitas e zircoes das minas de Morro Velho e Passagem de Mariana – Quadrilátero Ferrífero (MG). In: 39 Congresso Brasileiro de Geologia, Sociedade Brasileira de Geologia, Abstract 6, pp. 470–472.

Schrank, A., Machado, N., 1996. Idades U-Pb em monazitas e zircoes do distrito aurifero de Caete, da Mina de Cuiaba e do Deposito de Carrapato-Quadrilatero Ferrifero (MG). In: 39 Congresso Brasileiro de Geologia, Sociedade Brasileira de Geologia, Abstract 6, pp. 473–475.

Scott, D.J., St-Onge, M.R., 1995. Constraints on Pb closure temperature in titanite based on rocks from the Ungava orogen, Canada: Implications for U-Pb geochronology and P–T–t path determinations. Geology 23 (12), 1123–1126.

Seixas, L.A.R., David, J., Stevenson, R., 2012. Geochemistry, Nd isotopes and U-Pb geochronology of a 2350 Ma TTG suite, Minas Gerais, Brazil: implications for the crustal evolution of the southern São Francisco craton. Precambr. Res. 196–197, 61–80.

Seixas, L.A.R., Bardintzeff, J.-M., Stevenson, R., Bonin, B., 2013. Petrology of the high-Mg tonalites and dioritic enclaves of the ca. 2130 Ma Alto Maranhão suite: evidence for a major juvenile crustal addition event during the Rhyacian orogenesis, Mineiro Belt, southeast Brazil. Precambr. Res. 238, 18–41.

Silva, M.G., 1992. Evidências Isotópicas e Geocronológicas de um Fenômeno de Acrescimento Crustal Transamazônico no Cráton do São Francisco, Estado da Bahia. In: 37 Congresso Brasileiro de Geologia, São Paulo, Brazil. Sociedade Brasileira de Geologia, Abstract 2. pp. 181–182.

Silva, M.G., Martin, H., Abram, M.B., 1996. Datação do corpo máfico-ultramáfico da fazenda Mirabela (Ipiaú–Ba) pelo método Sm–Nd: Implicações petrogenéticas e geotectônicas. In: *39 Congresso Brasileiro de Geolodia, Salvador, Brazil*, pp. 217–220.

Silva, L.C., McNaughton, N.J., Melo, R.C., Fletcher, I.R., 1997. U-Pb SHRIMP ages in the Itabuna-Caraiba TTG high-grade complex: the first window beyond the Paleoproterozoic overprint of the eastern Jequié Craton, NE Brazil. In: International Symposium on Granites and Associated Mineral. ISGAM, Salvador, Bahia, Brazil, pp. 282–283.

Silva, M.G., Silva Coelho, C.E., Teixeira, J.B.G., Alves da Silva, F.C., Bras de Souza, J.A., Silva, R.A., 2001. The Rio Itapicuru greenstone belt, Bahia, Brazil: geologic evolution and review of gold mineralisation. Miner. Deposita 36, 345–357.

Silva, L.C., Armstrong, R., Noce, C.M., Carneiro, M.A., Pimentel, M., Pedrosa-Soares, A.C., Leite, C.A., Vieira, V.S., Silva, M.A., Paes, V.J.C., Cardoso Filho, J.M., 2002. Reavaliação da evolução geológica em terrenos pré-cambrianos brasileiros com base em novos dados U-Pb Shrimp, Parte II: Orógeno Araçuaí, Cinturão Mineiro e Craton São Francisco meridional. Rev. Bras. Geociências 32, 513–528.

Silva, L.C., Pedrosa-Soares, A.C., Armstrong, R., Pinto, C.P., Magalhães, T.R., Pinheiro, M.A.P., Santos, G.G., 2015. Disclosing the Paleoarchean to Ediacaran history of the São Francisco craton basement: The Porteirinha domain (northern Araçuaí orogen, Brazil). J. S. Am. Earth Sci. http://dx.doi.org/10.1016/j.jsames.2015.12.002.

Tassinari, C.C.G., Mateus, A.M., Velásquez, M.E., Munhá, J.M.U., Lobato, M.L., Bello, R.M., Chiquini, A.P., Campos, W.F., 2015. Geochronoloy and thermochronology of gold mineralization in the Turmalina deposit, NE of the Quadrilátero Ferrífero Region, Brazil. Ore Geol. Rev. 67, 368–381.

Teixeira, W., 1985. A evolução geotectônica da porção meridional do Craton do São Francisco, com base em interpretações geocronológicas. Unpublished Ph.D. Thesis Insitute of Geosciences, University of São Paulo, São Paulo, Brazil. 207.

Teixeira, W., Figueiredo, M.C.H., 1991. An outline of early proterozoic crustal evolution in the São Francisco region, Brazil: a review. Precambr. Res. 53, 1–22.

Teixeira, W., 1996. The Mantiqueira metamorphic complex, Eastern Minas Gerais State: preliminary geochronological and geochemical results. Anais da Acad. Bras. de Ciências 68, 223–246.

Teixeira, W., Onstott, T.C., Makenya, M., Szabó, G.A.J., 1996. Proterozoic thermochronologic implications from 40Ar/39Ar and K-Ar dating of the Campo Belo metamorphic complex, Southern São Francisco Craton, Brazil. Anais da Acad. Bras. de Ciências 69 (1), 59–75.

Teixeira, W., Sabaté, P., Barbosa, J., Noce, C.M., Carneiro, M.A., 2000. Archean and Paleoproterozoic Evolution of the São Francisco Craton, Brazil. In: Cordani, U.G., Milani, E.J., Thomaz Filho, A., Campos, D.A. (Eds.). Tectonic Evolution of South America, Rio de Janeiro, pp. 101–137. 31 IGC.

Teixeira, W., Ávila, C.A., Dussin, I.A., Corrêa Neto, A.V., Bongiolo, E.M., Santos, J.O., Barbosa, N.S., 2015. A juvenile accretion episode (2.35–2.32 Ga) in the Mineiro Belt and its role to the Minas accretionary orogeny: Zircon U-Pb–Hf and geochemical evidences. Precambr. Res. 256, 148–169.

Toledo, C.L.B., 2002. Evolução geológica das rochas máficas e ultramáficas no Greenstone Belt Barbacena, na região de Nazareno M>G>. Unpublished Ph.D. Thesis Instituto de Geociências - Universidade Estadual de Campinas, Campinas, Brazil. 307.

Vavra, G., Gebauer, D., Schmidt, D., Compston, W., 1996. Multiple zircon growth and recrystallization during polyphase Late Carboniferous to Triassic metamorphism in granulites of the Ivrea Zone (Southern Alps): an ion microprobe (SHRIMP) study. Contrib. Miner. Petrol. 122, 337–358.

Vavra, G., Schaltegger, U., 1999. Post-granulite facies monazite growth and rejuvenation during Permian to Lower Jurassic thermal and fluid events in the Ivrea Zone (Southern Alps). Contrib. Miner. Petrol. 134, 404–414.

Vasconcelos, P., Becker, T., 1992. A idade da mineralização aurífera no depósito da Fazenda Brasileiro, Bahia, Brasil. Pesquisas atuais e novas tendências. Universidade Estadual de Campinas, Bol. Res, Workshop em Metalogênese, 29.

Verts, L., Chamberlain, K.R., 1996. U-Pb sphene dating of metamorphism: the importance of sphene growth in the contact aureole of the Red Mountain pluton, Laramie Mountains, Wyoming. Contr. Min. Petrol. 125, 186–199.

Vlach, S.R.F., Campos Neto, M.C., Caby, R., Basei, M.A.S., 2003. Contact metamorphism in metapelites from the Nova Lima Group, Rio das Velhas Supergroup, Quadrilátero Ferrífero: A monazite Th–U–Pbt dating by the electron-probe microanalyser. In: *IV South American Symposium on Isotope Geology*, Vol. I, pp. 307–310.

Williams, I.S., Buick, I.S., Cartwright, I., 1996. An extended episode of early Mesoproterozoic metamorphic fluid flow in the Reynolds Range, central Australia. J. Metamorph. Geol. 14, 29–47.

Williams, I.S., 2001. Response of detrital zircon and monazite, and their U-Pb isotopic systems, to regional metamorphism and host-rock partial melting, Cooma Complex, southeastern Australia. Aust. J. Earth Sci. 48, 557–580.

Wilson, N., 1987. Combined Sm-Nd, Pb-Pb and Rb-Sr geochronology and Isotope Geochemistry in Polymetamorphic Precambrian Terrains: Examples from Brazil and Channel IslandU.K.. Unpublished Ph.D. Thesis Oxford University, United Kingdom. 250.

Zuccheti, M., Lobato, L.M., Baltazar, O.F., 2000. Volcanic and volcaniclastic features in Archean rocks and their tectonic environment, Rio das Velhas Greenstone Belt, Quadrilátero Ferrífero, MG-Brazil. Rev. Bras. de Geociências 30, 388–392.

Zuccheti, M., Lobato, L.M., Baars, F.J., 2000. Genetically diverse basalt geochemical signatures developed in the Rio das Velhas Greenstone Belt, Quadrilátero Ferrífero, Minas Gerais, Brazil. Rev. Bras. de Geociências 30, 397–402.